

**A practical guide to the solution
of real-life optimal control problems**

by

Hans Josef Pesch

Mathematisches Institut
Technische Universität München
München,
Germany

The present paper is an introductory and survey paper of the treatment of realistically modelled optimal control problems from applications in the aerospace field. Especially those problems are considered which include different types of constraints. In the tutorial part of the paper, recipes are given for the treatment of optimal control problems for which, among other constraints, control and/or state variable inequality constraints are to be taken into account. Optimal control problems having singular subarcs and/or discontinuities are also investigated. The discussion of the necessary conditions aims to the subsequent application of the multiple shooting method, which is known to be a very precise and efficient method for the solution of those multipoint boundary-value problems that arise from these necessary conditions. Homotopy techniques as well as the fusion of direct collocation and multiple shooting techniques are described. Both approaches facilitate the construction of an appropriate initial trajectory to start the multiple shooting iteration. In the survey part of the paper, some recently published new guidance methods are described. These methods are based, on the one hand, on the theory of neighboring extremals and, on the other hand, on the multiple shooting method. They are designed for the real-time computation of optimal trajectories in aerospace applications. Five challenging optimal control problems from the field of aerospace engineering run throughout the whole paper and illustrate the use of the recipes, i.e., the necessary conditions that must be satisfied by an optimal solution. Numerical results are given for these problems to demonstrate the performance of the multiple shooting method for the off-line computation of optimal trajectories as well as the performance of the guidance schemes for the on-line computation of optimal trajectories.

Keywords : Optimal control problems, necessary conditions, control variable inequality constraints, state variable inequality constraints, singular subarcs, multipoint boundary-value problems,

multiple shooting, homotopy techniques, fusion of direct and indirect methods, neighboring extremals, feedback controls, real-time computation, on-line computation, re-entry problems, windshear problems, two-stage-to-orbit ascent.

1. Introduction

Many optimization problems in science and engineering can be described by optimal control problems such as the control of a spacecraft or aircraft, of a chemical reaction or of an industrial robot. Thereby, the consideration of different constraints is very important when realistic models are to be solved. Such complex optimal control problems can today be treated by sophisticated numerical methods. If the accuracy of the solution and the judgement of its optimality holds the spotlight, the multiple shooting method seems to be superior over other methods. The complexity of optimal control problems that have been solved by the multiple shooting method until now also contributes to this assessment. Some of these problems may be cited here: the maximum payload ascent of a new generation of space transportation systems known as the Sanger II project (partly published, currently still under research), maximum payload missions by ion-driven spacecrafts to planetoids or outer planets (results just published), the dangerous landing of a passenger aircraft in a wind-shear downburst (results just published), optimal heating and cooling by solar energy (already published), and time or energy optimal control of robots (partly published, still under research). The present investigations and the results obtained clearly show the trend that control problems are treated of which the mathematical models become closer and closer to reality. This causes an increase of complexity of optimal control problems by an increasing number of constraints, by more complicated differential equations, which themselves must be even generated by a computer program and, finally, also by an increasing number of unknowns that are involved in the model.

The present survey paper looks out for two aims. First, the necessary conditions of optimal control theory are summarized in a short course; see Sections 2-6. Thereby, special emphasis is placed on the treatment of inequality constraints which must be taken into account when real-life applications are treated. Each section starts with a summary of the necessary conditions, which can be used as a recipe. For simplicity, the mathematical background is omitted completely. This may help to get some insight in what kind of routine work has to be done to solve an optimal control problem that fits into the rather general pattern of the problems discussed here. The summary is then followed by the discussion of a realistic problem from the field of aerospace engineering. At the end of each section, the resulting boundary-value problem is given which provides the basis for the subsequent numerical solution by means of the multiple shooting method. This method and homotopy techniques as well as a new idea to unify

direct and indirect methods are described in Sections 7 and 8.

After this tutorial material, a survey is given on some new methods for the real-time computation of optimal trajectories. This is the second intention of the present paper. For, if optimal solutions of processes which run down very fast, such as the optimal flight of space vehicles or aircrafts, are to be realized practically, it is not sufficient just to prescribe the initial data and leave the process to its fate. Instead, one needs a fast numerical method to compute the future course of the optimal control variables during the process so that optimality conditions and prescribed constraints are preserved even in the presence of disturbances. These requirements can be met by guidance schemes that are based on the theory of neighboring extremals. Based on this theory, the flight path corrections can be obtained from the solutions of linear boundary-value problems which can be solved very efficiently. A first method, a so-called neighboring optimum guidance scheme, needs only a few matrix-times-vector operations which have to be carried through on the onboard computer for the on-line computation of the corrections of the optimal control variables. The second method, called repeated correction method, combines this linear guidance law with a single integration of the equations of motion. By this method, not only the control corrections, but also the control history as well as the associated trajectory can be computed for the entire remaining flight time. In addition, the observance of the constraints can be verified before feeding back the adjusted control history. The theoretical and numerical background of these methods is covered in Sections 9-11.

In detail, the paper has the following outline. In Section 2, problems with control variable inequality constraints are discussed. The heating constraint re-entry of an Apollo capsula is investigated as an example. The constraint of the angle of attack represents the control variable inequality constraint in this example. Next, the maximum cross-range re-entry problem of a space-shuttle-orbiter-type vehicle provides the example for the treatment of mixed state-control constraints, where both control and state variables are involved. This kind of problems are discussed in Section 3. The treatment of state variable inequality constraints is explained in Section 4. Again, the heating constraint re-entry of an Apollo capsula serves as an example. Now, the altitude after the first dip into the atmosphere is limited because of safety requirements. This inequality constraint represents a second-order state constraint. Bang-bang and singular control problems are investigated in Section 5. The abort landing of a passenger aircraft in a windshear downburst serves as the example for this type of problems. Finally, problems with discontinuities of the state variables appearing in the performance index and in certain constraints are discussed in Section 6. The maximum payload ascent of a two-stage-to-orbit space transporter yields the illustrating example. All these challenging optimal control problems of different degree of difficulty may serve as a set of benchmark problems for numerical methods designed for the solution of real-life optimal control problems.

The multiple shooting method is described in brevity in Section 7 as well as homotopy techniques, which are very useful to overcome the obstacle of finding an appropriate initial guess for starting the multiple shooting iteration. Direct methods, such as direct collocation, can also be used to get the required initial trajectory. Some numerical results for all problems are presented in Section 8.

In Section 9, the theory of neighboring extremals is given in brevity. The description of the guidance methods is presented in Section 10. Some numerical results concerning the performance of these guidance schemes for the on-line computation of optimal trajectories are given in Section 11.

Section 12 concludes this introductory and survey paper.

2. Optimal control problems with control variable inequality constraints

2.1. Summary of necessary conditions

At the beginning of the tutorial part of the paper, we concentrate on the treatment of the following simple class of nonlinear optimal control problems. To be minimized is a functional

$$I[u] := \varphi(x(t_f), t_f) + \int_0^{t_f} L(x(t), u(t)) dt \quad (1)$$

over all piecewise continuous control vector functions $u : [0, t_f] \rightarrow U \subset \mathbb{R}^k$ where U denotes a non-empty, convex and closed set. The piecewise continuously differentiable state vector function $x : [0, t_f] \rightarrow \mathbb{R}^n$ is subject to the following constraints in form of a system of ordinary differential equations and of two-point boundary conditions,

$$\dot{x}(t) = f(x(t), u(t)) , \quad f : \mathbb{R}^{n+k} \rightarrow \mathbb{R}^n , \quad (2a)$$

$$x(0) = x_0 , \quad x_0 \in \mathbb{R}^n , \quad (2b)$$

$$\psi(x(t_f), t_f) = 0 , \quad \psi : \mathbb{R}^n \times \mathbb{R}_+ \rightarrow \mathbb{R}^q \quad (2c)$$

where the terminal time t_f may be either specified or unspecified. It is assumed that all functions appearing in Eqs. (1) and (2) are sufficiently often continuously differentiable with respect to their arguments.

In the following, some results of the theory of optimal control are summarized. The notation of Bryson and Ho 1987 is used to present the following necessary conditions which have to be satisfied by an optimal solution. Defining the Hamiltonian H and the auxiliary function Φ

$$H(x, u, \lambda) := L(x, u) + \lambda^T f(x, u) , \quad (3)$$

$$\Phi(x, t, \nu) := \varphi(x, t) + \nu^T \psi(x, t) , \quad (4)$$

an optimal solution of the problem (1) and (2) has to fulfill the necessary conditions

$$\dot{\lambda}^\top = -H_x, \quad (5a)$$

$$u = \arg \min_{u \in U} H, \quad (5b)$$

$$\lambda^\top(t_f) = \Phi_x|_{t_f}. \quad (5c)$$

If the terminal time t_f is unspecified, the following necessary condition has to be included,

$$(\Phi_t + H)|_{t_f} = 0. \quad (5d)$$

Here $\lambda : [0, t_f] \rightarrow \mathbb{R}^n$ and $\nu \in \mathbb{R}^q$ denote the so-called Lagrange multipliers or adjoint variables. The partial derivatives H_x and Φ_x are to be understood as row vectors, e.g., $H_x := (\partial H / \partial x_1, \dots, \partial H / \partial x_n)$, and the transpose of the column vector (\cdot) is denoted by $(\cdot)^\top$, e.g., $x^\top := (x_1, \dots, x_n)$.

2.2. Example: Apollo re-entry (version 1: constrained angle of attack)

A first optimal control problem is investigated now to illustrate the procedure of how to transform an optimal control problem by means of the above necessary conditions into a boundary-value problem that is well suited for a subsequent numerical treatment. This first problem describes the atmospheric re-entry of an Apollo-type capsula. Since different versions of this problem are so often published in the literature, see, e.g., Breakwell et. al. 1963, Scharmack 1967, and Stoer and Bulirsch 1980 and, more recently, Pesch 1989B, 1990A, it has become a benchmark problem for optimization methods. Its complexity is still low enough to serve as a tutorial example.

The flight path of the capsula is assumed to take place in a vertical plane. Thus, the equations of motion can be written as

$$\dot{V} = -\frac{S}{2m} \rho V^2 C_D(u) - \frac{g_0 \sin \gamma}{(1 + \xi)^2}, \quad (6a)$$

$$\dot{\gamma} = \frac{S}{2m} \rho V C_L(u) + \frac{V \cos \gamma}{R(1 + \xi)} - \frac{g_0 \cos \gamma}{V(1 + \xi)^2}, \quad (6b)$$

$$\dot{\xi} = \frac{V}{R} \sin \gamma, \quad (6c)$$

$$\dot{\zeta} = \frac{V}{1 + \xi} \cos \gamma. \quad (6d)$$

Here V denotes the velocity, γ the flight path angle, ξ the normalized altitude ($\xi := h/R$ with h and R denoting the altitude above the Earth's surface and the

Earth's radius, respectively), and ζ the distance on the Earth's surface. The control variable is the angle of attack u . For the lift and the drag coefficients, the following relations are assumed, $C_D(u) = C_{D_0} + C_{D_L} \cos u$ with $C_{D_0} = 0.88$ and $C_{D_L} = 0.52$ and $C_L(u) = C_{L_0} \sin u$ with $C_{L_0} = -0.505$. The air density is assumed to satisfy $\varrho = \varrho_0 \exp(-\beta R \xi)$. All other quantities not mentioned here are constants.

The total stagnation point convective heating per unit area, i.e.,

$$I[u] = \int_0^{t_f} 10 V^3 \sqrt{\varrho} dt \quad (7)$$

is to be minimized.

The vehicle is to be maneuvered into an initial position favorable for the final splashdown in the Pacific. Thus, all state variables are prescribed at the moment of entry. At the unspecified terminal time, all state variables except the flight path angle are prescribed, too. More details, especially the values of the constants and the boundary conditions, can be found in Pesch 1989B.

In addition, the range U of the control variable is described by the inequality constraint

$$|u| \leq u_{\max} \quad (8)$$

with a given positive constant $u_{\max} \leq \pi$. This completes the description of the model.

We now establish the necessary conditions of optimal control theory. In a first step, the optimal control variable is eliminated in terms of the state and the adjoint variables. If the optimal control variable lies in the interior of the set U , the following equations must be satisfied because of the minimum principle (5b),

$$H_u = 0, \quad (9a)$$

$$H_{uu} > 0. \quad (9b)$$

In the general case of more than one control variable, the strong Legendre-Clebsch condition (9b) is to be understood as H_{uu} must be a positive definite matrix. Because of technical reasons, there must hold $u \in [-\pi, \pi]$ here. The optimal control variable u is then given, according to Eq. (9a), by

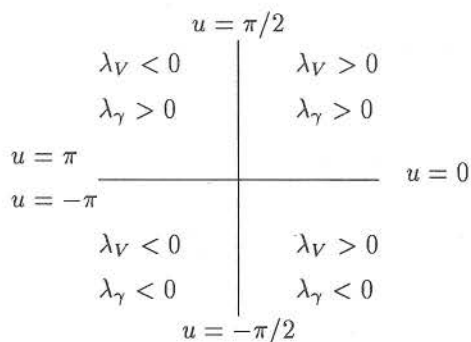
$$\tan u = -\frac{C_{L_0} \lambda_\gamma}{C_{D_L} V \lambda_V}. \quad (10)$$

By this condition, u is not uniquely defined. The quadrant is determined by Eq. (9b). We find $\text{sign } u = \text{sign } \lambda_\gamma$ or, in more detail,

$$\sin u = -C_{L_0} \frac{\lambda_\gamma}{\sqrt{(C_{D_L} V \lambda_V)^2 + (C_{L_0} \lambda_\gamma)^2}}, \quad (11a)$$

$$\cos u = +C_{D_L} \frac{V \lambda_V}{\sqrt{(C_{D_L} V \lambda_V)^2 + (C_{L_0} \lambda_\gamma)^2}}. \quad (11b)$$

The following diagram shows the relation between the quadrant of u and the signs of the adjoint variables λ_V and λ_γ ,



Note that the trajectory has a so-called corner at times t_{corner} where there holds $\lambda_\gamma(t_{\text{corner}}) = 0$ and $\lambda_V(t_{\text{corner}}) < 0$. This results in a jump of the optimal control variable from $-\pi$ to $+\pi$ or vice versa if $u_{\text{max}} = \pi$ is chosen for the maximum value of the control variable. In this case, the state variables, however, remain continuously differentiable. However, this is not true for $u_{\text{max}} < \pi$ as we will see. The trajectory then has, indeed, a corner since the flight path angle has a jump discontinuity at $t = t_{\text{corner}}$.

The adjoint variables can be computed via the Eqs. (5a), which are not given in detail here.

On constrained subarcs, where the control variable, if chosen according to Eqs. (11), would violate the inequality constraint (8), we have either $u = u_{\text{max}}$ or $u = -u_{\text{max}}$. The minimum principle (5b) yields $\text{sign } u = \text{sign } u^{\text{free}}$. Here, u^{free} denotes the competitive control variable, which is not active along constrained subarcs and determined by Eqs. (11). Hence, we have

$$u = u_{\text{max}} \text{sign } u^{\text{free}} \quad (12)$$

on constrained subarcs. At junction points between unconstrained and constrained subarcs, the control variable is continuous. However, there arises a discontinuity in the interior of a constrained subarc if λ_γ changes its sign, say at $t = t_{\text{corner}}$, while simultaneously there holds $\lambda_V(t_{\text{corner}}) < 0$. This is because u^{free} jumps at $t = t_{\text{corner}}$ from $-\pi$ to $+\pi$ or vice versa depending on the sign of $\lambda_\gamma(t_{\text{corner}})$; see the above diagram. Note that the Erdmann-Weierstraß corner condition yields the continuity of λ , H , and H_u at $t = t_{\text{corner}}$; see, e.g., Bryson and Ho 1987, p. 125.

Finally, the set of necessary conditions is completed with the so-called transversality conditions (5c) and (5d),

$$\lambda_\gamma(t_f) = 0, \quad (13a)$$

$$H|_{t_f} = 0. \quad (13b)$$

Note that γ is the only state variable not prescribed at the terminal time t_f , i.e., $\Phi_\gamma = 0$. The adjoint vector ν drops out.

2.3. The multipoint boundary-value problem

In summary, the entire set of necessary conditions yields a multipoint boundary-value problem. To achieve the so-called standard form of the boundary-value problem, we have to transform the undetermined interval $[0, t_f]$ onto the interval $[0, 1]$ by introducing a new independent variable τ via $\tau := t/t_f$. Then, t_f becomes a new dependent variable and, because of $(\cdot)' := \frac{d}{d\tau}(\cdot) = t_f \frac{d}{dt}(\cdot) := t_f \frac{d}{dt}(\cdot)$, the right-hand sides of Eqs. (6) as well as of Eqs. (5a) are to be multiplied by t_f . Hence, we have a system of 9 differential equations (the differential equation for the unknown terminal time is given by $t_f' = 0$) with 9 two-point boundary conditions (7 boundary conditions are given by the model, 2 conditions follow from the transversality conditions (13)). In addition, each junction point $t = t_{\text{junction}}$ between unconstrained and constrained subarcs yields an interior boundary condition of type

$$u^{\text{free}}(t_{\text{junction}}) \pm u_{\text{max}} = 0. \quad (14)$$

Corners are also determined by an interior boundary condition,

$$\lambda_\gamma(t_{\text{corner}}) = 0 \quad (15)$$

if, in addition, there holds

$$\lambda_V(t_{\text{corner}}) < 0. \quad (16)$$

By this procedure, the necessary conditions are transformed into a multipoint boundary-value problem which can be solved by the multiple shooting method very accurately and efficiently; see Section 7. Note that a solution of the above boundary-value problem is not a candidate for an optimal solution of the control problem if the inequality (8) and the sign conditions $\text{sign } u = \text{sign } u^{\text{free}}$ and (16) are not fulfilled along the entire trajectory or at all corner points t_{corner} , respectively.

3. Optimal control problems with mixed state-control inequality constraints

3.1. Summary of necessary conditions

Realistically modelled problems generally include inequality constraints of more complicated type than Eq. (8). At the first level of increased complexity, we consider so-called mixed state-control constraints of type

$$C(x(t), u(t)) \leq 0, \quad C: \mathbb{R}^{n+k} \rightarrow \mathbb{R}^l \quad (17)$$

where C explicitly depends on the control vector u , i.e., $C_u \neq 0$. For the sake of simplicity, we firstly restrict the following explanations to the case $k = l = 1$, thus one control variable and one inequality constraint. Defining the Hamiltonian by

$$H(x, u, \lambda, \mu) := L(x, u) + \lambda^\top f(x, u) + \mu C(x, u), \quad (18)$$

the necessary conditions (5) remain unchanged. Additionally we have a necessary sign condition for the Lagrange parameter μ ,

$$\mu \begin{cases} = 0 & \text{if } C < 0, \\ \geq 0 & \text{if } C = 0. \end{cases} \quad (19)$$

Therefore, the right-hand sides of the differential equations for the adjoint variables (5a) are, in general, to be modified along constrained subarcs, where

$$C(x, u) = 0 \text{ for all } t \text{ with } t_{\text{entry}} \leq t \leq t_{\text{exit}} \text{ and } t_{\text{entry}} < t_{\text{exit}}. \quad (20)$$

The moments $t = t_{\text{entry}}$ and $t = t_{\text{exit}}$ denote entry and exit point, respectively, of a constrained subarc. If Eq. (20) can be uniquely solved for u , i.e., if $C_u \neq 0$, the control variable can be represented along a constrained subarc by a function of the state variables,

$$u = u^{\text{bound}}(x). \quad (21)$$

If $C_u \neq 0$, the multiplier μ is given by means of Eq. (9a),

$$\mu = -C_u^{-1} \cdot (L_u + \lambda^\top f_u). \quad (22)$$

If $k > 1$ or $l > 1$, but each component of C depends explicitly on one control vector component only, this case can be treated by adding terms in the definition (18) of the Hamiltonian. If one control vector component is constrained by several components of C , this problem can be reduced to the previous problem by introducing a new surrogate inequality constraint. The single case that has to be excluded because of its possible non-uniqueness is the case where one component of C depends explicitly on several control vector components. This case is of minor practical importance only and cannot be treated with sufficient generality.

3.2. Example: space-shuttle re-entry under a heating constraint

For illustration purposes, we consider a second example from the aerospace field. The following optimal control problem describes the maximal cross-range re-entry of a space-shuttle-type vehicle. Increased range capacity of the vehicle allows more frequent returns from the orbit. The functional to be minimized is the negative cross-range angle at the unspecified terminal time t_f ,

$$I[u] = -\Lambda(t_f). \quad (23)$$

Assuming no planet rotation and oblateness, a stationary atmosphere, a point mass vehicle, and a constant drag polar, the equations of motion with respect to a flight-path-oriented coordinate system may be written as

$$\dot{V} = -(C_{D_0} + C_L^n) \frac{F \rho_0}{2m} \exp(-\beta h) V^2 - g_0 \left(\frac{R}{R+h} \right)^2 \sin \gamma, \quad (24a)$$

$$\dot{\chi} = C_L \frac{F \rho_0}{2m} \exp(-\beta h) V \frac{\sin \kappa}{\cos \gamma} - \frac{V}{R+h} \cos \gamma \cos \chi \tan \Lambda, \quad (24b)$$

$$\dot{\gamma} = C_L \frac{F \rho_0}{2m} \exp(-\beta h) V \cos \kappa - \left(\frac{g_0}{V} \left(\frac{R}{R+h} \right)^2 - \frac{V}{R+h} \right) \cos \gamma, \quad (24c)$$

$$\dot{\Lambda} = \frac{V}{R+h} \cos \gamma \sin \chi, \quad (24d)$$

$$\dot{h} = V \sin \gamma, \quad (24e)$$

$$\dot{\Theta} = \frac{V}{R+h} \frac{\cos \gamma \cos \chi}{\cos \Lambda}. \quad (24f)$$

The state variables are the velocity V , the heading angle χ , the flight path angle γ , the cross-range angle Λ , the altitude h , and the down-range angle Θ . The control variables are the bank angle κ and the lift coefficient C_L . The values of the constants of the drag polar are $C_{D_0} = 0.04$ and $n = 1.86$.

Initial values for all state variables are prescribed as well as terminal conditions for V , γ , and h . Since the differential equation for the down-range angle Θ is decoupled, it need not be considered for the optimization process and can be computed afterward.

Moreover, the following mixed state-control or zeroth order state constraint has to be taken into account, which limits the skin temperature of the vehicle,

$$C_L - C_{LH}(V, h) - \Delta C_{LH} \leq 0 \quad (25)$$

where C_{LH} is a rather complicated function of V and h consisting of 20 terms each of which is the sum of a polynomial of second degree in V/h plus a polynomial of second degree in h/V multiplied by a polynomial of first degree in h . Different levels of the limit skin temperature T are indicated by the parameter ΔC_{LH} where $\Delta C_{LH} = 0$ corresponds to a limit skin temperature of $T = 1093^\circ\text{C}$. For details, see Kugelmann and Pesch 1990B.

According to Eqs. (9), the optimal control variables are given by

$$\sin \kappa = -\lambda_\chi / (w \cos \gamma), \quad \cos \kappa = -\lambda_\gamma / w, \quad (26)$$

where

$$w = [(\lambda_\chi / \cos \gamma)^2 + \lambda_\gamma^2]^{1/2},$$

and

$$C_L = \begin{cases} C_L^{\text{free}} := [-w/(V \lambda_V n)]^{1/(n-1)}, & \text{on unconstrained arcs,} \\ C_L^{\text{bound}} := C_{LH}(V, h) + \Delta C_{LH}, & \text{on constrained arcs.} \end{cases} \quad (27)$$

Note that Eq. (9b) is fulfilled if $H_{\kappa\kappa} > 0$ and $H_{\kappa\kappa} H_{C_L C_L} - H_{\kappa C_L}^2 > 0$. This obviously implies $H_{C_L C_L} > 0$, too. From these inequalities, which are to be satisfied on unconstrained subarcs only, we obtain an additional sign condition that must be fulfilled along unconstrained subarcs,

$$\lambda_V < 0. \quad (28a)$$

Note that the above determinant condition is trivially satisfied for the parameter values of the problem.

For mixed state-control constraints, the right-hand sides of the adjoint variables are to be modified along constraint subarcs; see Eq. (5a) together with the definition (18). For the sake of brevity, we give here the equation for λ_h only,

$$\begin{aligned} \dot{\lambda}_h = - \left\{ \lambda_V \left[(C_{D_0} + k C_L^n) \frac{F \varrho_0}{2m} \exp(-\beta h) V^2 + 2 \frac{g_0 R^2}{(R+h)^3} \sin \gamma \right] \right. \\ + \lambda_\chi \left[-C_L \frac{F \varrho_0}{2m} \beta \exp(-\beta h) V \frac{\sin \kappa}{\cos \gamma} \right. \\ \left. + \frac{V}{(R+h)^2} \cos \gamma \cos \chi \tan \Lambda \right] \\ + \lambda_\gamma \left[-C_L \frac{F \varrho_0}{2m} \beta \exp(-\beta h) V \cos \kappa \right. \\ \left. + \left(2 \frac{g_0 R^2}{(R+h)^3} V - \frac{V}{(R+h)^2} \right) \cos \gamma \right] \\ \left. + \lambda_\Lambda \left[-\frac{V}{(R+h)^2} \cos \gamma \sin \chi \right] - \mu \frac{\partial C_{LH}}{\partial h} \right\} \end{aligned}$$

where the Lagrange parameter μ is defined by Eq. (9a),

$$\mu = \begin{cases} 0, & \text{on unconstrained arcs,} \\ \frac{F \varrho_0}{2m} \exp(-\beta h) V [w + V \lambda_V n C_L^{n-1}], & \text{on constrained arcs.} \end{cases}$$

The necessary sign condition (19) implies

$$\lambda_V \geq -\frac{w}{V n C_L^{n-1}} (< 0) \quad (28b)$$

which must be fulfilled on constrained subarcs and therefore completes the sign condition (28a).

Finally, the missing boundary conditions are given by the transversality conditions (5c) and (5d),

$$\lambda_x(t_f) = 0, \quad \lambda_\Lambda(t_f) = -1, \quad H|_{t_f} = 0. \quad (29)$$

3.3. The multipoint boundary-value problem

In summary, we have again a multipoint boundary-value problem which must be solved by a candidate for the optimal trajectory. We have 11 differential equations for V , χ , γ , Λ , h , their associate adjoint variables, and for t_f . In contrast to the boundary-value problem of Subsection 2.3, the right-hand sides are piecewise defined here. In addition, 8 two-point boundary conditions are given by the model, and 3 terminal conditions are given by the above transversality conditions. Each entry or exit point, t_{entry} or t_{exit} , respectively, of the mixed state-control constraint (25) is determined by an interior condition of the type

$$[C_L^{\text{free}} - C_{LH}(V, h) - \Delta C_{LH}] \Big|_{t_{\text{entry/exit}}} = 0. \quad (30)$$

If the down-range angle Θ is to be computed, too, its differential equation is also included together with an appropriate initial value.

After the computation of the solution of the boundary-value problem, the solution must be checked whether the inequalities (25) and (28) are satisfied.

At the end of this section, it should be mentioned that control variable inequality constraints of type $C(u(t)) < 0$, which are treated in Section 2, fit also into the above pattern. Because of $C_x = 0$, the differential equations for the adjoint variables need not be modified in this case, and μ therefore need not be computed, in order to establish the boundary-value problem. However, the sign condition (19) must be verified.

4. Optimal control problems with state variable inequality constraints

4.1. Summary of necessary conditions

The next degree of complexity is given by optimal control problems with state variable inequality constraints,

$$S(x(t)) \leq 0, \quad S: \mathbb{R}^n \rightarrow \mathbb{R}^{\bar{l}}. \quad (31)$$

In the following, we summarize some results of optimal control theory for problems with state variable inequality constraints. For the sake of simplicity, let us

assume that $k = \bar{l} = 1$. We first consider the case that the constraint is active on a non-vanishing subinterval $[t_{\text{entry}}, t_{\text{exit}}]$,

$$S(x(t)) \equiv 0 \quad \text{for all } t \in [t_{\text{entry}}, t_{\text{exit}}] \subset [0, t_f]. \quad (32)$$

By successive differentiation of (32) with respect to time and substituting (2a), we find the smallest non-negative number \bar{q} such that there holds

$$S(x) \equiv 0, \quad S^{(1)}(x) \equiv 0, \quad \dots, \quad S^{(\bar{q}-1)}(x) \equiv 0 \quad \text{on } [t_{\text{entry}}, t_{\text{exit}}] \quad (33a)$$

and

$$S^{(\bar{q})}(x, u) \equiv 0 \quad \text{with} \quad S_u^{(\bar{q})}(x, u) \neq 0. \quad (33b)$$

Here, $S^{(i)}$ denotes the i -th total time derivative of S . Then, \bar{q} is called the order of the state constraint. Now $S^{\bar{q}}(x, u)$ plays the role of $C(x, u)$ in (18) so that the Hamiltonian, in this case, is defined by

$$H(x, u, \lambda, \mu) = L(x, u) + \lambda^\top f(x, u) + \mu S^{\bar{q}}(x, u). \quad (34)$$

Again, for μ we have the necessary sign condition

$$\mu \begin{cases} = 0, & \text{if } S < 0, \\ \geq 0, & \text{if } S = 0. \end{cases} \quad (35)$$

On constrained arcs, we obtain the optimal control variable u from (33b) and μ from (9a). The right-hand sides of the differential equations for the adjoint variables (5a) are, in general, to be modified on $[t_{\text{entry}}, t_{\text{exit}}]$. In order to guarantee that not only (33b) but also (33a) is satisfied, we also have to require that the so-called entry or tangency conditions are fulfilled,

$$N^\top(x(t_{\text{entry}}, t_{\text{entry}})) := (S(x(t_{\text{entry}})), S^{(1)}(x(t_{\text{entry}})), \dots, S^{(\bar{q}-1)}(x(t_{\text{entry}}))) = 0. \quad (36)$$

Alternatively, the tangency conditions can also be posted at the exit point. The following explanations have then to be modified suitably.

Interior point conditions of the type

$$N(x(t_{\text{interior}}, t_{\text{interior}})) = 0, \quad N : \mathbb{R}^n \times (0, t_f) \rightarrow \mathbb{R}^{\bar{q}} \quad (37)$$

give rise to additional necessary conditions,

$$\lambda^\top(t_{\text{interior}}^+) = \lambda^\top(t_{\text{interior}}^-) - \pi^\top N_x |_{t_{\text{interior}}}, \quad (38a)$$

$$H(t_{\text{interior}}^+) = H(t_{\text{interior}}^-) + \pi^\top N_t |_{t_{\text{interior}}} \quad (38b)$$

where $\pi \in \mathbb{R}^{\bar{q}}$ denotes another Lagrange multiplier. The Eq. (38b) determines t_{interior} , and the \bar{q} components of π are chosen so that the interior point constraint (37) is satisfied. The multiplier π influences (37) via the differential

equations indirectly by the jump condition (38a). The generalization to interior point conditions at several points t_{interior} is obvious.

From the tangency conditions (36) holding at the entry point of a constrained subarc, we have that λ generally is discontinuous at $t = t_{\text{entry}}$ whereas λ is continuous at the exit point t_{exit} . In case the tangency conditions are placed at the exit point, this result holds vice versa.

Sometimes boundary or touch points occur instead of boundary arcs. If, for example, the order is $\bar{q} = 2$, the following conditions hold at a touch point t_{touch} ,

$$S(x(t_{\text{touch}})) = 0, \quad S^{(1)}(x(t_{\text{touch}})) = 0. \quad (39)$$

The first condition is regarded as an interior point condition of type (37) and yields a possible discontinuity of λ . The second condition determines the touch point t_{touch} .

Minimax or so-called Chebyshev optimal control problems also fit into the pattern of state-constrained optimal control problems; see Section 5.

4.2. Example: Apollo re-entry (version 2: constrained altitude)

To illustrate the use of the above extended set of necessary conditions, we again consider the re-entry problem of Subsection 2.2. Now, we replace the control variable inequality constraint (8) by the state variable inequality constraint

$$\xi \leq \xi_{\max} \quad (40)$$

which has, because of safety reasons, to be taken into account after the first dip into the atmosphere, i.e., for all $t > t_{\min}$ for which $\gamma(t_{\min}) = 0$ for the first time. Here, ξ_{\max} is a given positive constant.

One easily finds by successive differentiation of $S(x(t)) := \xi(t) - \xi_{\max}$ with respect to time t that the state constraint is of the second order, thus $\bar{q} = 2$. The optimal control variable is given on a constrained subarc by

$$\sin u = \frac{2m}{F \varrho C_{L_0}} \left(\frac{g_0}{V^2 (1 + \xi_{\max})^2} - \frac{1}{R(1 + \xi_{\max})} \right). \quad (41a)$$

Note that $S^{(1)} \equiv 0$ and $S^{(2)} \equiv 0$ imply $\dot{\gamma} \equiv 0$. The optimal control variable along a constrained subarc is uniquely determined by the minimum principle (5b) from which follows

$$\text{sign } \cos u = \text{sign } \lambda_V. \quad (41b)$$

By an indirect proof, it can be shown that there holds $\cos u \neq 0$ on $]t_{\text{entry}}, t_{\text{exit}}[$. This directly implies that $S^{(2)}(x, u) = 0$ can be solved for u on the entire open interval $]t_{\text{entry}}, t_{\text{exit}}[$. Since $\lambda_V(t_{\text{entry}}) < 0$ implies $\lambda_V(t) < 0$ on $]t_{\text{entry}}, t_{\text{exit}}[$, which can also be proved indirectly, the control variable is continuous on $]t_{\text{entry}}, t_{\text{exit}}[$. Because of the continuity of the Hamiltonian, see Eq. (38b), it follows that \dot{V} and $\dot{\gamma}$ are continuous at the junction points t_{entry} and t_{exit} unless, at these

points, there holds $\lambda_V = 0$ and $\lambda_\gamma = 0$ as well. If this case is disregarded, $S^{(2)}$ and also u are continuous at the junction points, too.

In case of a constrained subarc, the entry conditions (36) yield

$$\xi(t_{\text{entry}}) = \xi_{\max} , \quad (42a)$$

$$\gamma(t_{\text{entry}}^-) = 0 \quad (42b)$$

where the minus sign at t_{entry} indicates that the control variable is to be chosen according to Eqs. (11). Because of the continuity of the control variable at the junction points, it follows

$$u^{\text{free}}(t_{\text{entry}}) = u^{\text{bound}}(t_{\text{entry}}) \quad (42c)$$

$$u^{\text{free}}(t_{\text{exit}}) = u^{\text{bound}}(t_{\text{exit}}) \quad (42d)$$

where u^{free} is defined by the Eqs. (11) and u^{bound} by the Eqs. (41). The present case is completed by the jump conditions

$$\lambda_\gamma(t_{\text{entry}}^+) = \lambda_\gamma(t_{\text{entry}}^-) - \pi_1 , \quad \pi_1 \in \mathbb{R} , \quad (43a)$$

$$\lambda_\xi(t_{\text{entry}}^+) = \lambda_\xi(t_{\text{entry}}^-) - \pi_2 , \quad \pi_2 \in \mathbb{R} . \quad (43b)$$

In summary, the 4 additional unknowns t_{entry} , t_{exit} , π_1 , and π_2 are determined by the 4 interior boundary conditions (42). The above jump conditions have to be carried through at the entry point of the constrained subarc and cause that the Lagrange parameters π_1 and π_2 have influence on the solution of the system of differential equations. The right-hand sides of the adjoint variables are to be modified along a constrained subarc; compare Section 3.

It is known from the literature that state constraints of even order may have boundary arcs as well as touch points if the Hamiltonian is regular, i.e., if H has a unique minimum with respect to u in a small neighborhood of the optimal trajectory for all $t \in [0, t_f]$. Moreover, it is known that state constraints of the first order do not become active in form of touch points; only boundary arcs occur. Furthermore, for state constraints of odd order with $\bar{q} > 3$, only touch points occur; boundary arcs are impossible. Proofs for these results can be found in Jacobson et. al. 1971.

Hence, we here have to take into account the appearance of touch points, too. According to Eqs. (39), we have two conditions at a touch point t_{touch} ,

$$\xi(t_{\text{touch}}) = \xi_{\max} , \quad (44a)$$

$$\gamma(t_{\text{touch}}) = 0 . \quad (44b)$$

The first of these conditions is considered as an interior point constraint and gives rise to a jump condition,

$$\lambda_\xi(t_{\text{touch}}^+) = \lambda_\xi(t_{\text{touch}}^-) - \pi , \quad \pi \in \mathbb{R} . \quad (45)$$

The second condition (44b) determines the touch point. The Lagrange parameter π must be chosen so as to satisfy the interior point constraint (44a).

In case that several boundary arcs and several touch points exist, the above interior boundary conditions and their associated jump conditions must be multiplied suitably. If a boundary arc is adjacent to $t = 0$ or $t = t_f$, either the Eqs. (42a)–(42c) and (43) or Eq. (42d) have to be dropped. In the latter case, it is advisable to reduce the number of unknowns in the boundary-value problem by placing the jump conditions at $t = t_f$ since they can be neglected then.

4.3. The multipoint boundary-value problem

For the version of the re-entry problem with the altitude constraint, the terminal flight path angle is prescribed, so that the terminal condition (13a) must be cancelled. In summary, we have again a system of 9 differential equations with a corresponding number of two-point boundary conditions. In addition, there are 4 interior boundary conditions for each interior boundary arc by which the 4 unknowns, entry and exit point and the two jump parameters π_1 and π_2 , are determined. For each touch point, there are 2 interior boundary conditions by which the touch point and the jump parameter π is determined. Thus, we have now a different type of a multipoint boundary-value problem which includes, because of the Eqs. (43) and (45), jump conditions, too.

In addition, necessary sign conditions concerning both the Lagrange parameter μ and its time derivatives up to the order \bar{q} and the jump parameter vector π must be fulfilled by an optimal solution. By these necessary conditions, which are based on Jacobson et. al. 1971 and Maurer 1976, non-optimal solutions can be singled out; see, e.g., Bulirsch et. al. 1991A where a summary of those sign conditions can be found. These necessary conditions can be written for the present re-entry problem as

$$\dot{\mu} \leq 0, \quad \ddot{\mu} \geq 0, \quad (46a)$$

$$\pi_1 \geq 0, \quad \pi_2 \geq 0, \quad \pi \geq 0. \quad (46b)$$

At the end of this section, it should be mentioned that control variable inequality constraints of type $C(x(t), u(t)) < 0$, which are treated in Section 3, fit also into the above pattern; they can be considered as zeroth order state constraints. No discontinuities arise for the adjoint variables if $\bar{q} = 0$.

5. Optimal control problems with singular subarcs

5.1. Summary of necessary conditions

Among the most complicated optimal control problems, we have problems where the control variables appear linearly in both the functional and the equations of motion. The difficulties are caused by the fact that the control variables may

have so-called singular subarcs. The treatment of those singular subarcs will be explained in the following.

We refer to the general formulation of the optimal control problem in Section 2.1. Let us assume that at least one control variable appears linearly in Eqs. (1) and (2a) and that the set U mentioned after Eq. (1) is a compact and convex polyhedron which is indeed the case in most practical problems. For the sake of simplicity, let $k = 1$ and $U = [u_{\min}, u_{\max}]$. Then, the Hamiltonian has the form

$$H(x, u, \lambda) := A(x, \lambda) + u B(x, \lambda) .$$

If the term $B(x, \lambda)$ does not vanish identically on a non-vanishing subinterval $[t_{\text{entry}}, t_{\text{exit}}]$ of $[0, t_f]$, the minimum principle (5b) yields

$$u = \begin{cases} u_{\max}, & \text{if } B < 0 , \\ u_{\min}, & \text{if } B > 0 . \end{cases} \quad (47)$$

In this case, we have so-called bang-bang subarcs only. Each isolated zero of the switching function $S(t) := B(x(t), \lambda(t))$ indicates a switch from $u = u_{\max}$ to $u = u_{\min}$ or vice versa.

If

$$B(x, \lambda) \equiv 0 \quad \text{for all } t \in [t_{\text{entry}}, t_{\text{exit}}] \subset [0, t_f] , \quad t_{\text{entry}} < t_{\text{exit}} , \quad (48)$$

singular subarcs occur. The optimal control variable on these singular subarcs can be computed in a similar way as for state-constrained problems. By successive differentiation of the switching function S with respect to time t and the substitution of the Eqs. (2a) and (5a), we may find a smallest positive integer \bar{q} such that

$$S^{(\bar{q})}(x, u, \lambda) \equiv 0 \quad \text{for all } t \in [t_{\text{entry}}, t_{\text{exit}}] \quad (49a)$$

and

$$S_u^{(\bar{q})}(x, u, \lambda) \neq 0 . \quad (49b)$$

If such a smallest integer \bar{q} exists, it must be even; see McDanell and Powers 1971. Therefore, p with $\bar{q} = 2p$ is called the order of the singular subarc. The case of most practical interest is $p = 1$ which will be considered here only. The control variables near singular subarcs of higher order generally show a chattering behavior. According to McDanell and Powers 1971, the control variable u is, for first-order singular control problems, either discontinuous or continuously differentiable at the junction points t_{entry} and t_{exit} . The first case occurs in general. The analogon to the strong Legendre-Clebsch condition (9b) for singular subarcs is the so-called strong generalized Legendre-Clebsch condition, see Kelley et. al. 1967, which reads as

$$(-1)^p B_{2p}(x, \lambda) > 0 \quad \text{for } t_{\text{entry}} \leq t \leq t_{\text{exit}} \quad (50)$$

where $B_{2p}(x, \lambda)$ is the factor in front of u after $2p$ differentiations of the identity (48).

The interior boundary conditions to determine bang-bang switching points $t = t_{\text{bang}}$ and entry and exit points of singular subarcs are given either by isolated zeros of the switching function

$$S(t_{\text{bang}}) = 0 \quad (51)$$

or by two tangency conditions, either by

$$S(t_{\text{entry}}) = 0, \quad S^{(1)}(t_{\text{entry}}) = 0 \quad (52a)$$

or by

$$S(t_{\text{entry}}) = 0, \quad S(t_{\text{exit}}) = 0. \quad (52b)$$

Jump conditions do not occur here. Again, we obtain well-defined multipoint boundary-value problems. Each bang-bang switching point t_{bang} is determined by an equation of type (51). Each pair of an entry and an exit point of singular subarcs are determined by equations of type (52a) or (52b).

5.2. Example: abort landing of a Boeing 727 in a windshear downburst

For illustration purposes, we consider here the problem of abort landing of a passenger aircraft in the presence of a windshear downburst which is taken from Miele et. al. 1987 and Bulirsch et. al. 1991A. This is one of the most complicated optimal control problems ever solved. Here, we will discuss the treatment of the bang-bang and singular subarcs only which indeed appear in the candidate trajectory for the optimal solution of the problem.

To set up the equations of motion, we assume that the aircraft is a particle of constant mass, the flight takes place in a vertical plane, and Newton's law is valid in an Earth-fixed system. Moreover, the wind flow field is assumed to be steady. Under these assumptions, the kinematical and dynamical equations are

$$\dot{x} = V \cos \gamma + W_x, \quad (53a)$$

$$\dot{h} = V \sin \gamma + W_h, \quad (53b)$$

$$\dot{V} = \frac{T}{m} \cos(\alpha + \delta) - \frac{D}{m} - g \sin \gamma - (\dot{W}_x \cos \gamma + \dot{W}_h \sin \gamma), \quad (53c)$$

$$\dot{\gamma} = \frac{T}{mV} \sin(\alpha + \delta) + \frac{L}{mV} - \frac{1}{V} g \cos \gamma + \frac{1}{V} (\dot{W}_x \sin \gamma - \dot{W}_h \cos \gamma), \quad (53d)$$

$$\dot{\alpha} = u. \quad (53e)$$

The state variables are the horizontal distance x , the altitude h , the relative velocity V , and the relative path inclination γ . In the formulation above, the

relative angle of attack α is regarded as a state variable, too. In fact, its time derivative is chosen as control variable. The approximations of the aerodynamic forces, the thrust $T = T(V, \beta)$, the drag $D = D(V, \alpha)$, and the lift $L = L(V, \alpha)$, as well as the prescribed wind velocity components $W_x(x)$ and $W_h(x, h)$ can be found in Bulirsch et. al. 1991A. The power setting β , normally also a control variable, is specified in advance as a function of time; see, e.g., Bulirsch et. al. 1991A. All other quantities not mentioned here explicitly are constants and given also in Bulirsch et. al. 1991A.

The following inequality constraints are imposed on the problem

$$|u| \leq u_{\max} , \quad (54a)$$

$$\alpha \leq \alpha_{\max} . \quad (54b)$$

The second constraint is a state constraint of the first order and can be treated analogously to the re-entry problem of Section 4.2. For the boundary conditions see, e.g., Bulirsch et. al. 1991A. The terminal time t_f is unspecified here, too.

To avoid crashing on the ground, the ground clearance, or in other words the minimal altitude, has to be maximized,

$$\max_{u \in U} \min_{0 \leq t \leq t_f} h(t) .$$

Here, U is described by the control variable inequality constraint (54a). Instead, we can also minimize the peak value of the altitude drop, that is, the difference between a constant reference altitude h_R and the instantaneous altitude,

$$I[u] := \max_{0 \leq t \leq t_f} \{h_R - h(t)\} . \quad (55)$$

The reference altitude h_R has to be chosen so as to satisfy $h_R \geq h(t)$ for all $t \in [0, t_f]$. In any case, we have a so-called Chebyshev-type optimal control problem, which can be transformed into the standard form of a Mayer's functional by introducing a new state variable. For the functional (55) define

$$\zeta(t) := \max_{0 \leq t \leq t_f} \{h_R - h(t)\} . \quad (56)$$

The variable ζ is now subject to the additional constraints

$$\dot{\zeta} = 0 , \quad (57a)$$

$$h_R - h(t) - \zeta(t) \leq 0 . \quad (57b)$$

The functional (55) can then be written in standard form

$$\bar{I}[u] = \zeta(t_f) . \quad (58)$$

Note that the transformation brings a new state constraint into the game which can be shown to be of the third order. The treatment can also follow the lines

of Section 4. For details, see also Bulirsch et. al. 1991A. Note that this abort landing problem presents an example with a non-regular Hamiltonian so that the theoretical results concerning boundary points and boundary arcs induced by state constraints do not apply here.

As mentioned above, we restrict the investigations to the computation of the control variable for state-unconstrained subarcs only to demonstrate the use of the necessary conditions for bang-bang and singular subarcs. From the minimum principle (5b), we obtain a bang-bang expression for the optimal control variable,

$$u = \begin{cases} u_{\max} & , \text{ for } \lambda_{\alpha} < 0 \\ -u_{\max} & , \text{ for } \lambda_{\alpha} > 0 \end{cases} \quad (59)$$

The adjoint variable λ_{α} plays the role of the switching function. Its isolated zeros,

$$\lambda_{\alpha}(t_{\text{bang}}) = 0 \quad , \quad (60)$$

mark the switches of the bang-bang subarcs. If non-isolated zeros of λ_{α} occur, the following relation holds,

$$\lambda_{\alpha}(t) \equiv 0 \quad \text{on } t_{\text{entry}} \leq t \leq t_{\text{exit}} \quad , \quad t_{\text{entry}} < t_{\text{exit}} \quad . \quad (61)$$

Repeating twice the differentiation of this identity with respect to time and substituting Eqs. (53) and (5a), we obtain an expression for the optimal control on singular subarcs,

$$u_{\text{sing}} = -\frac{A_{\text{sing}}}{B_{\text{sing}}} \quad , \quad (62)$$

with

$$\begin{aligned} A_{\text{sing}}(t) := & \dot{\lambda}_V [T \sin(\alpha + \delta) + D_{\alpha}] - \frac{1}{V} [\dot{\lambda}_{\gamma} - \lambda_{\gamma} \frac{\dot{V}}{V}] [T \cos(\alpha + \delta) + L_{\alpha}] \\ & + \lambda_V [\dot{T} \sin(\alpha + \delta) + D_{\alpha V} \dot{V}] - \lambda_{\gamma} \frac{1}{V} [\dot{T} \cos(\alpha + \delta) + L_{\alpha V} \dot{V}] \quad , \end{aligned}$$

$$B_{\text{sing}}(t) := \lambda_V [T \cos(\alpha + \delta) + D_{\alpha\alpha}] - \lambda_{\gamma} \frac{1}{V} [L_{\alpha\alpha} - T \sin(\alpha + \delta)] \quad .$$

Hence, the order of the singular control is $p = 1$, and the strong generalized Legendre-Clebsch condition is

$$B_{\text{sing}} < 0 \quad \text{for } t_{\text{entry}} \leq t \leq t_{\text{exit}} \quad . \quad (63)$$

The two junction points are determined by the entry or tangency conditions, either by

$$\lambda_{\alpha}(t_{\text{entry}}) = 0 \quad , \quad \dot{\lambda}_{\alpha}(t_{\text{entry}}) = 0 \quad (64a)$$

or by

$$\lambda_{\alpha}(t_{\text{entry}}) = 0 \quad , \quad \lambda_{\alpha}(t_{\text{exit}}) = 0 \quad . \quad (64b)$$

5.3. The multipoint boundary-value problem

Again, we see that the necessary conditions lead to a well-defined multipoint boundary-value problem. Each switching point t_{bang} , t_{entry} , or t_{exit} is accompanied by an interior boundary condition. For the complete description of the boundary-value problem, it is referred to Bulirsch et. al. 1991A.

If realistic models are investigated, characteristic parameters of the system are often given by tabular data. In this case, possible points of non-smoothness of the approximation of the data must be considered as interior point constraints of type (37), too. This causes additional switching points where the adjoint variables may have discontinuities. See Bulirsch et. al. 1991A for details.

6. Optimal control problems with discontinuities in the state variables

6.1. Summary of necessary conditions

Problems with discontinuities in the state variables at undetermined interior points where instead of (1) a functional of the form

$$\bar{I}[u] := \bar{\varphi}(x(t_{\text{stage}}^-), x(t_{\text{stage}}^+), x(t_f), t_f) + \int_0^{t_f} L(x(t), u(t)) dt \quad (65)$$

is to be minimized subject to the additional equality constraint

$$\bar{\psi}(x(t_{\text{stage}}^-), x(t_{\text{stage}}^+)) = 0, \quad \bar{\psi} : \mathbb{R}^{2n} \rightarrow \mathbb{R}^n, \quad (66)$$

lead to the additional necessary conditions

$$H|_{t_{\text{stage}}^-} = H|_{t_{\text{stage}}^+}, \quad (67a)$$

$$\lambda^\top(t_{\text{stage}}^\pm) = \mp \frac{\partial \bar{\Phi}}{\partial x(t_{\text{stage}}^\pm)} \quad (67b)$$

where

$$\bar{\Phi}(x^-, x^+, x, t, \bar{\nu}) := \bar{\varphi}(x^-, x^+, x, t) + \bar{\nu}^\top \bar{\psi}(x^-, x^+).$$

These equations determine x and λ at the discontinuity $t = t_{\text{stage}}$, the parameters $\bar{\nu} \in \mathbb{R}^n$ and the staging time t_{stage} . If one or more of the quantities t_{stage} , $x_i(t_{\text{stage}}^+)$ and $x_i(t_{\text{stage}}^-)$ are specified, the corresponding equations in (67a) and (67b) are omitted. A generalization to more discontinuities is obvious.

6.2. Example: ascent of a two-stage-to-orbit vehicle

The Sanger II project of a European space transportation system is, at present, in the focus of industrial and scientific discussion and development. In the future, a completely reusable space transportation system will be necessary to maintain and service cost-efficiently the planned international space station.

The two-stage-to-orbit vehicle is designed to launch horizontally and to deliver either a manned or an unmanned cargo unit into orbit. The first stage is equipped with wings and airbreathing engines. The second stage is conventionally rocket propelled. The system is capable of performing cruising flights.

Some ideas for such a space transportation system have already been developed by Eugen Sanger in the thirties. His investigations were republished in 1962; see Sanger 1962.

The first mathematical model which included a simultaneous staging and trajectory optimization for a two-stage rocket propelled predecessor model goes back to Shau 1973. A generalization to a three-dimensional model was presented by Bulirsch and Chudej 1991, 1992A. Recently the model was upgraded to include the airbreathing engines of the lower stage; see Bulirsch and Chudej 1992B and Chudej to appear.

The payload of the space transporter is to be maximized,

$$m_{\text{payload}} = m(t_f) - \Psi_{\text{II}}(m(t_{\text{stage}}^+) - m(t_f)) \quad (68)$$

subject to the stage separation condition

$$m(t_{\text{stage}}^+) = m(t_{\text{stage}}^-) - \Psi_{\text{I}}(m_0 - m(t_{\text{stage}}^-)) . \quad (69)$$

Here, t_{stage} denotes the unspecified time of separation of the two stages. The terminal time t_f is also unspecified. The functions Ψ_{I} and Ψ_{II} describe the structural mass consisting of the engines and the fuel tank in dependence of the fuel used for the two stages. For details, see Bulirsch and Chudej 1992A and Chudej to appear.

The equations of motion in a flight path oriented coordinate system over a spherical Earth with no wind in the atmosphere are

$$\begin{aligned} \dot{V} = \frac{1}{m} [T(V, h; b) \cos \epsilon - D(V, h; u)] - g(h) \sin \gamma \\ + \omega^2 (R + h) \cos \Lambda (\sin \gamma \cos \Lambda - \cos \gamma \sin \chi \sin \Lambda) , \end{aligned} \quad (70a)$$

$$\begin{aligned} \gamma = \frac{1}{mV} [T(V, h; b) \sin \epsilon + L(V, h; u)] \cos \kappa \\ - \left[\frac{g(h)}{V} - \frac{V}{R+h} \right] \cos \gamma + 2\omega \cos \chi \cos \Lambda \\ + \omega^2 \frac{R+h}{V} \cos \Lambda (\sin \gamma \sin \chi \sin \Lambda + \cos \gamma \cos \Lambda) , \end{aligned} \quad (70b)$$

$$\dot{\chi} = \frac{1}{mV \cos \gamma} [T(V, h; b) \sin \epsilon + L(V, h; u)] \sin \kappa \quad (70c)$$

$$\begin{aligned} & - \frac{V}{R+h} \cos \gamma \cos \chi \tan \Lambda \\ & + 2\omega (\sin \chi \cos \Lambda \tan \gamma - \sin \Lambda) \\ & - \omega^2 \frac{R+h}{V \cos \gamma} \cos \Lambda \sin \Lambda \cos \chi, \end{aligned}$$

$$\dot{h} = V \sin \gamma, \quad (70d)$$

$$\dot{\Lambda} = \frac{V}{R+h} \cos \gamma \sin \chi, \quad (70e)$$

$$\dot{\Theta} = \frac{V}{(R+h) \cos \Lambda} \cos \gamma \cos \chi, \quad (70f)$$

$$\dot{m} = -b. \quad (70g)$$

The state variables are the velocity V , the path inclination γ , the azimuth inclination χ , the altitude h , the geographical latitude Λ , the geographical longitude Θ , and the mass m . The control variables are the angle of attack u , the lateral inclination angle κ , the mass flow b , and the thrust angle ϵ . The formulae for the thrust T , the drag D , the lift L , and the gravitational acceleration $g(h)$ can be found in Bulirsch and Chudej 1992A. All other quantities are assumed to be constant.

The mass flow for both stages is subject to the constraints

$$0 \leq b \leq b_{I, \max} \quad \text{for } 0 \leq t \leq t_{\text{stage}}, \quad (71a)$$

$$0 \leq b \leq b_{II, \max} \quad \text{for } t_{\text{stage}} < t \leq t_f. \quad (71b)$$

For the boundary conditions, see Bulirsch and Chudej 1992A and Chudej to appear.

We concentrate here on the necessary conditions which are brought into the game by the stage separation condition and the functional including a discontinuity of the mass. According to Eqs. (67), the stage separation time t_{stage} is determined by the continuity condition of the Hamiltonian; see Eq. (67a). In addition, the adjoint variable λ_m has a jump discontinuity at $t = t_{\text{stage}}$,

$$\lambda_m(t_{\text{stage}}^+) = -\Psi'_{II}(m(t_{\text{stage}}^+) - m(t_f)) + \frac{\lambda_m(t_{\text{stage}}^-)}{1 + \Psi'_I(m_0 - m(t_{\text{stage}}^-))} \quad (72)$$

In contrast to the jump conditions introduced by state constraints, this jump condition describes a jump of fixed size which must be carried through at $t = t_{\text{stage}}$.

6.3. The multipoint boundary-value problem

Due to the constraint describing the stage separation, the dimension of the boundary-value problem is increased only by 1 to determine the unknown stage separation time. The constraint (69) yields a jump condition for the adjoint variable λ_m which must be taken into account together with the jump condition for the mass given by that Eq. (69). Both jump conditions do not contain any additional parameters to be determined as part of the solution of the problem as in Section 4.

7. Off-line computation of optimal trajectories by multiple shooting

7.1. Description of the method

As we have seen in the preceding sections, the necessary conditions of optimal control theory lead to a multipoint boundary-value problem of the following form

$$\dot{z}(t) = F(t, z(t)) = \begin{cases} F_0(t, z(t)), & 0 \leq t \leq \tau_1, \\ \vdots \\ F_s(t, z(t)), & \tau_s \leq t \leq t_f, \end{cases} \quad (73a)$$

$$z(\tau_k^+) = \Sigma_k(\tau_k, z(\tau_k^-)), \quad 1 \leq k \leq s, \quad (73b)$$

$$r_i(z(0), z(t_f)) = 0, \quad 1 \leq i \leq n_1, \quad (73c)$$

$$r_i(\tau_{k_i}, z(\tau_{k_i}^-)) = 0, \quad n_1 + 1 \leq i \leq N. \quad (73d)$$

The piecewise defined differential equations (73a) include the equations of motion, the system of differential equations for the adjoint variables, and some so-called trivial differential equations of form $\dot{z}_j = 0$, e.g., for jump parameters entering the jump conditions (73b). These jump conditions are brought into the problem by possible discontinuities of the adjoint variables when taking into account state variable inequality constraints. Equations (73c) and (73d) contain the prescribed boundary conditions for the state variables, the natural boundary conditions from the transversality conditions for the adjoint variables and for the terminal time if unspecified, and interior conditions, e.g., junction conditions for boundary or singular subarcs. All these conditions together determine not only the state and adjoint variables but also the switching times τ_k and the additional auxiliary variables, namely, the jump parameters mentioned above. The index k_i in the interior conditions serves as an indicator as to whether switching conditions are associated with a single switching point or not. The piecewise defined right-hand side of (73a) is based on an assumption of an

optimal switching structure associated with a sequence of switching points and their corresponding control laws between every pair of adjacent switching or boundary points, respectively.

In addition, there are sign conditions which the components z_j have to satisfy. These conditions must be checked after the solution of the boundary-value problem is computed. Non-optimal candidates can therewith be singled out.

A large class of optimal control problems fit into this pattern when analyzing the necessary conditions of optimal control theory. This kind of multipoint boundary-value problem is especially well suited for the well-known multiple shooting method (see, e.g., Bulirsch 1971 and Stoer and Bulirsch 1980). A new version was developed by Oberle 1982 and the most recent FORTRAN code, called BNDSO, is published in the user manual of Oberle and Grimm 1989.

In the following, we give a brief survey of the multiple shooting method with special emphasis on applications to multipoint boundary-value problems with jump conditions.

The multiple shooting method requires a fixed subdivision of the time interval which has to be chosen by the user,

$$0 =: t_1 < t_2 < \dots < t_m := t_f, \quad (74)$$

with $t_j \neq \tau_k$, $j = 1, \dots, m$ and $k = 1, \dots, s$. Initial data for the variables z_i at the times t_j have to be guessed as well as the switching points τ_k . Let the initial guess be $Z_j^{(0)}$ for the vectors $z(t_j)$ and $\tau^{(0)}$ for $\tau := (\tau_1, \dots, \tau_s)^T$. These data will be changed iteratively. The superscript for the iteration counter will be dropped in the following. Incidentally, the choice of the partition of the interval is rather uncritical. If possible, the grid should be finer in regions of stronger changes of the variables, whereas it can be coarser in other parts.

The basic idea of multiple shooting is to reduce the boundary-value problem to a series of initial-value problems: For $j = 1, \dots, m-1$, find the numerical solution of the initial-value problems

$$\dot{\bar{z}}(t) = \begin{bmatrix} F(t, z(t)) \\ 0 \end{bmatrix}, \quad t_j \leq t \leq t_{j+1}, \quad \text{with } \bar{z}(t_j) = \bar{Z}_j := \begin{bmatrix} Z_j \\ \tau \end{bmatrix}, \quad (75)$$

where $\bar{z}(t) := (z(t), \tau)^T$. During the numerical integration, the jump conditions (73b) have to be carried out at the switching points $\tau_k \in [t_j, t_{j+1}]$. Moreover, the integration must be stopped at the switching points, even if no jumps have to be performed. In general, higher derivatives of some variables have discontinuities here, which may reduce the order of convergence of the integration method. Note that the right-hand side F changes with k .

Let $\bar{z}(t; t_j, \bar{Z}_j) = (z(t; t_j, \bar{Z}_j), \tau)^T$ denote the solution of the initial-value problem (75) in the interval $[t_j, t_{j+1}]$. Then, a trajectory $z(t)$ and the associated switching points τ_k are a solution of the above multipoint boundary-value problem if and only if the vector $\bar{Z} := (\bar{Z}_1, \dots, \bar{Z}_{m-1})^T$ is a zero of

$$\mathcal{F}(\bar{Z}) = 0. \quad (76)$$

Here, the components of \mathcal{F} include the continuity or matching conditions

$$\mathcal{F}_j(\bar{Z}_1, \dots, \bar{Z}_{m-1}) := \bar{z}(t_{j+1}; t_j, \bar{Z}_j) - \bar{Z}_{j+1}, \quad 1 \leq j \leq m-2, \quad (77a)$$

and the boundary and switching conditions

$$\mathcal{F}_{m-1}(\bar{Z}_1, \dots, \bar{Z}_{m-1}) := \begin{bmatrix} R(\bar{Z}_1, \bar{Z}_{m-1}) \\ Q(\bar{Z}_1, \dots, \bar{Z}_{m-1}) \end{bmatrix}, \quad (77b)$$

with

$$R(\bar{Z}_1, \bar{Z}_{m-1}) := [r'_i(Z_1, z(t_m; t_{m-1}, \bar{Z}_{m-1}))]_{i=1, \dots, n_1},$$

$$Q(\bar{Z}_1, \dots, \bar{Z}_{m-1}) := [r_i(\tau_{\kappa_i}, z(\tau_{\kappa_i}^-; t_{\kappa_i}, \bar{Z}_{\kappa_i}))]_{i=n_1+1, \dots, N}.$$

The index κ_i is defined by $t_{\kappa_i} < \tau_{\kappa_i} < t_{\kappa_i+1}$.

The aforementioned code BNDSCO is basically an implementation of the modified Newton method to determine the zero of \mathcal{F} :

$$\bar{Z}^{(i+1)} = \bar{Z}^{(i)} - \rho^{(i)} D\mathcal{F}(\bar{Z}^{(i)})^{-1} \mathcal{F}(\bar{Z}^{(i)}), \quad i = 0, 1, \dots \quad (78)$$

Here $\rho^{(i)}$ denotes the relaxation parameter of the i -th iteration step. This modified Newton method is characterized by the following features: The Jacobian matrix $D\mathcal{F}$ is approximated either via numerical differentiation or via an appropriate Broyden update. For details, see Stoer and Bulirsch 1980, pp. 266–270. The Broyden update is applied only during the iteration phase in which the iteration enters the final phase of quadratic convergence. Moreover, the Newton method is based on a relaxation strategy according to Deuffhard 1975 using a sophisticated test function check to increase the domain of convergence. In addition, a so-called rank strategy is incorporated to handle ill-conditioned problems; see Deuffhard 1974. These techniques yield a robust algorithm benefitting from the advantage of Newton's method, its quadratic convergence. The disadvantage is the rather small domain of convergence which, however, is assuaged by the use of homotopy techniques as explained in the following paragraph. In each Newton iteration, the solution of the system of linear equations is via Householder transformations taking into account the sparse structure of the coefficient matrix. Details can be found in Section 10.1, too. The magnitude of the norm of that matrix indicates the sensitivity of the solution at t_m with respect to the initial values at t_1 . The norm and condition number of the coefficient matrix can be estimated from the Householder decomposition matrices. This is a very useful information assessing the course of the iteration process. By the way, the elimination of unknowns in the boundary-value problem, if possible, may reduce the condition number of the boundary-value problem considerably.

7.2. Homotopy techniques

For the application of the multiple shooting method, the switching structure has to be guessed and initial guesses for all variables have to be provided. This seems

to be a strong restriction when applying the method. However, the construction of a so-called homotopy chain is a powerful tool to overcome these obstacles. By a homotopy chain, we understand the construction of a family of problems, *naturally* related to the problem to be solved, so that at least one member of that family can be treated easily. Let that family be associated with a real parameter, say ω . So we have to solve, according to Eq. (76), a one-parameter family of systems of nonlinear equations

$$\mathcal{F}(\bar{Z}; \omega) = 0, \quad \omega_{\text{initial}} \leq \omega \leq \omega_{\text{final}}.$$

The solution of a “simpler” problem, say for $\omega = \omega_i$, can then be used as initial guess for the “next” problem, say for $\omega = \omega_{i+1}$. Here, we make an ad hoc choice of the homotopy stepsize $\Delta\omega := \omega_{i+1} - \omega_i$. The starting point for this homotopy chain is $\omega = \omega_{\text{initial}}$ and it terminates with $\omega = \omega_{\text{final}}$. It is very important that ω is a *natural* parameter of the problem. Otherwise, this procedure might fail. It must be mentioned that the family of problems generally includes various classes of subproblems, with each class consisting of a one-parameter family of subsubproblems in such a way that the “last” problem of the class j is identical to the “first” problem of the class $j + 1$. This means that we may have to switch from one homotopy parameter to another when changing the class. We call this a homotopy strategy.

To illustrate this procedure, we take again the windshear problem from Section 5.2 and show how the third-order state constraint (57b) is introduced step by step. Because the functional

$$J[u] := \int_0^{t_f} (h_R - h(t))^{2r} dt, \quad (79)$$

approximates the Chebyshev functional (55) for $r \rightarrow \infty$; see, e.g., Bulirsch et al. 1991A, we first solve the approximating optimal control problem using that functional and choosing $r = 3$. Then, we combine the two functionals by

$$\mathfrak{S}[u] := (1 - \omega) \cdot \int_0^{t_f} (h_R - h(t))^6 dt + \omega \cdot \zeta(t_f) \quad (80)$$

and solve a whole chain of optimal control problems by varying the homotopy parameter ω from $\omega = 0$ to $\omega = 1$. By this procedure, the state constraint (57b) is introduced step by step into the problem. A solution of each problem in the chain of solutions serves as initial guess for the solution of the next problem which is to be solved until $\omega = 1$ is reached. For details see Bulirsch et al. 1991B. Note that the approach via the functional (80) is successful here since the Chebyshev functional (55) and the Bolza functional (79) are related in a natural way. The coupling of two problems which are not related to each other in a similar way as by Eq. (80) will generally fail to succeed.

Actually, this is the procedure to treat all aforementioned problems. First, the unconstrained problem is solved unless the control problem requires the consideration of the inequality constraints to be well-defined. Hence, for the abort landing problem the control variable inequality constraint (54a) must be taken into account from the very beginning of the homotopy. In the subsequent steps of the procedure, the inequality constraints are tightened. Graphical output devices help to detect, for example, whether a touch point splits into two touch points or into a boundary arc. This is the common behavior for second-order state constraints; see the numerical results for the altitude-constrained Apollo re-entry problem in Section 8.3. The appearance of a singular subarc can be detected when the switching function tends to oscillate around zero during the course of a homotopy run; see, e.g., also Bulirsch et. al. 1991B and Section 8.4.

A useful and easy-to-apply homotopy technique is described in Deuffhard et. al. 1976 and the recipe is given here for the example of the Space-Shuttle re-entry. The limit skin temperature can be influenced in a natural way by the parameter ΔC_{LH} ; see Eq. (25). If we introduce the homotopy parameter $\omega := \Delta C_{LH}$ as additional unknown into the boundary-value problem with the differential equation

$$\omega = 0, \quad (81a)$$

the boundary condition

$$\omega(t_f) = \omega_{i+1} := \Delta C_{LH}^{\text{new}}, \quad (81b)$$

and the initial guess

$$\omega^{(0)}(t) \equiv \omega_i := \Delta C_{LH}^{\text{old}}, \quad (81c)$$

the convergence of the modified Newton method (78) with an initial relaxation factor $\rho^{(0)} < 1$ can be accelerated considerably. The matching conditions are obviously fulfilled then. The only defect occurs in the two-point boundary condition for ω . However, this approach may not work in all cases. It can be shown that, when using this approach, the first iterate of the Newton method is tangential to the homotopy path, and the relaxation strategy of the modified Newton method provides a homotopy stepsize control; see Deuffhard et. al. 1976 for details.

7.3. Combination of direct and indirect methods

Nevertheless, the construction of an appropriate initial trajectory even for the unconstrained problems remains often a difficult and time-consuming problem. Many numerical experiments are sometimes needed for the solution of different test initial-value problems since, in general, no information precise enough is available about the adjoint variables. Recently, a method was developed which combines a direct collocation method with the multiple shooting method; see

von Stryk and Bulirsch 1992. Based on the approximate solution of the optimal control problem provided by the direct collocation method, initial estimates can be also obtained for the Lagrange multipliers λ from the adjoint variables of the Lagrangian of the nonlinear programming problem which is obtained via parameterization of the optimal control problem and by using collocation techniques. First numerical experiences show that the approximation yielded by the direct collocation method is accurate enough to obtain convergence with the multiple shooting iteration, if the problem is still simple enough. This means the problem must not include inequality constraints; see Bulirsch et al. to appear. So, homotopy techniques still must be used. By this fusion of direct and indirect methods, one can benefit from the superior accuracy provided by the multiple shooting method, and the disadvantage caused by the small domain of convergence of the multiple shooting method is considerably diminished. Moreover, direct collocation is a very efficient method because no integration of differential equations is to be carried out; the right-hand sides of the differential equations are to be fulfilled pointwise only. On the other side, the disadvantage of direct methods, namely that numerical solutions may be obtained that are not optimal, do not play a role if checked by an indirect method afterward.

8. Numerical results I

Numerical results for all aforementioned problems can be found in the literature. Therefore, the results are not repeated here in detail. Instead, some of the difficulties occurring during the process of solving the different optimal control problems are discussed. In addition, a few components of the optimal solutions are given here to have the major results at hand and to know how the optimal solutions look like.

8.1. Minimum heating re-entry of an Apollo capsule under a constraint of the angle of attack

The optimal solutions of the re-entry problem with the control variable inequality constraint presented in Section 2 show eleven different classes of switching structures depending on the tightness u_{\max} of the the angle-of-attack constraint. Here, only two aspects shall be pointed out. The first difficulty that arises after the construction of a starting trajectory for the control-unconstrained problem is described by the question how the switching structure will look like if the constraint is tightened slightly only. Starting from the optimal control history for $u_{\max} = 180$ deg, see Fig. 1, it seems to be manifest to expect one boundary subarc to appear at the end of the flight interval. Indeed, Fig. 2 represents the optimal solution due to $u_{\max} = 160$ deg obtained via 3 homotopy steps. The dashed line indicate the competitive nonactive unconstrained control denoted by u^{free} and determined by Eqs. (11). Note that λ_γ must have a zero at $t = t_f$;

see Eq. (13a). In the course of the next homotopy steps, it turns out that λ_γ becomes zero in the interior of the constrained subarc, too, while simultaneously λ_V is negative. Thus, a corner appears in the optimal solution. Figure 3 shows the control history for $u_{\max} = 118$ deg. The homotopy stepsize is $\Delta u_{\max} = 8$ deg when using the modified technique of Deuffhard et. al. 1976; compare Eqs. (81).

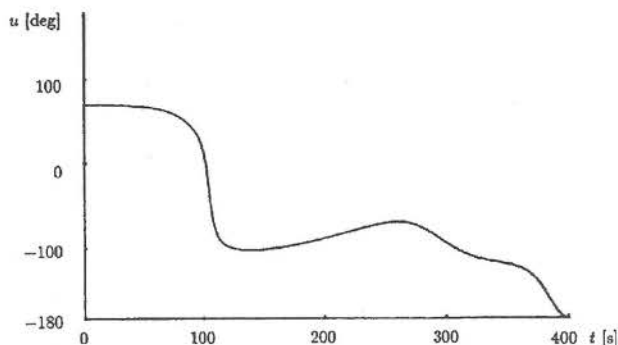


Figure 1. Control history for the Apollo re-entry; $u_{\max} = 180$ deg.

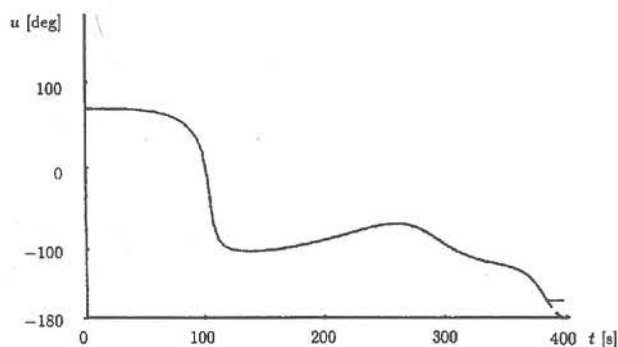


Figure 2. Control history for the Apollo re-entry; $u_{\max} = 160$ deg.

A further tightening of the constraint leads to the appearance of an additional subarc on the lower bound of the constraint near $t = 150$ sec, which then merges in the lower bound subarc ending at the corner; see Fig. 7 in Pesch 1989B. Next, an upper bound subarc occurs at the beginning of the flight time interval.

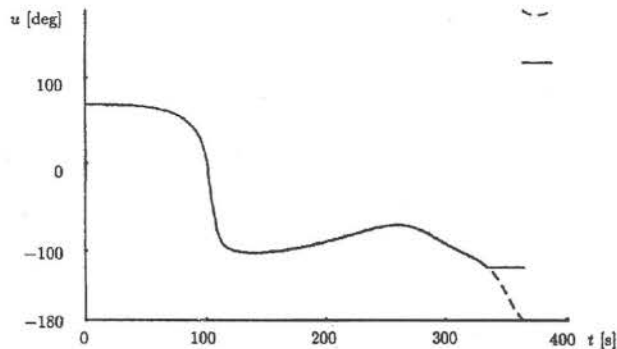


Figure 3. Control history for the Apollo re-entry; $u_{\max} = 118$ deg.

This situation is shown in Fig. 4 where $u_{\max} = 62$ deg. The homotopy stepsize decreases to $\Delta u_{\max} = 6$ deg.

During the next homotopy steps, the order of the zeros of λ_V and λ_γ changes: For $u_{\max} = 62$ deg, λ_γ has two zeros, say at $t = t_1$ and $t = t_5$, with $\lambda_\gamma < 0$ for $t_1 < t < t_5$, and λ_V has three zeros, say at $t = t_2$, $t = t_3$, and $t = t_4$, with $\lambda_V < 0$ for $t_2 < t < t_3$ and $t_4 < t$. All zeros are numbered with respect to their order. Thus, t_1 indicates $u = 0$, t_2 , t_3 , and t_4 indicate $u = -\pi/2$, and t_5 is just the corner point; compare Fig. 4. During the subsequent homotopy steps, the zeros t_2 and t_3 of λ_V disappear, i.e., $\lambda_V > 0$ for $t < t_4$, and the zero t_4 of λ_V moves beyond the zero t_5 of λ_γ . Hence, the discontinuous behavior of the optimal control disappears all of a sudden at a value $u_{\max} = u_{\max}^*$ where the problem becomes singular, i.e., the denominator in the Eqs. (11) becomes zero. The control history for $u_{\max} = 23$ deg, as a representative of the new class with a continuous optimal control, is given in Fig. 5.

Further results for $u_{\max} < 23$ deg are given in Pesch 1989B and Pesch 1990A. For this range of values, the homotopy stepsize decreases from $\Delta u_{\max} = 2$ deg to $\Delta u_{\max} = 0.1$ deg. The homotopy ends for $u_{\max} \approx 15.3$ deg having the switching structure $u = -u_{\max}$, $u = u^{\text{free}}$, $u = u_{\max}$ with the two switching points very closely side by side. The control variable inequality constraint reduces the maximal altitude gained by the re-ascent after the first dip into the atmosphere; see Figs. 9–11 in Pesch 1989B. Compare also Figs. 7 and 8.

By the way, the construction of a starting trajectory for a related re-entry problem where no inequality constraint is taken into account is described in Stoer and Bulirsch 1980. The solution of this problem provides the starting point for a homotopy towards the control-unconstrained problem of Section 2.2.

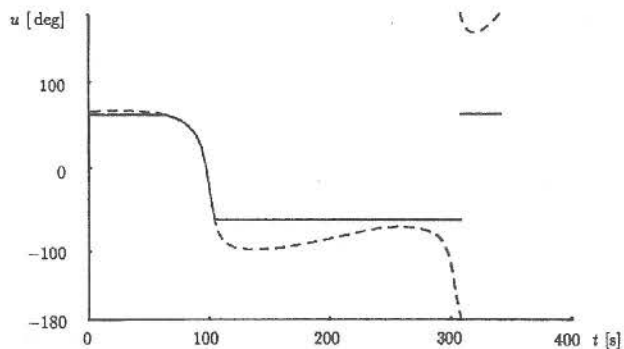


Figure 4. Control history for the Apollo re-entry; $u_{\max} = 62$ deg.

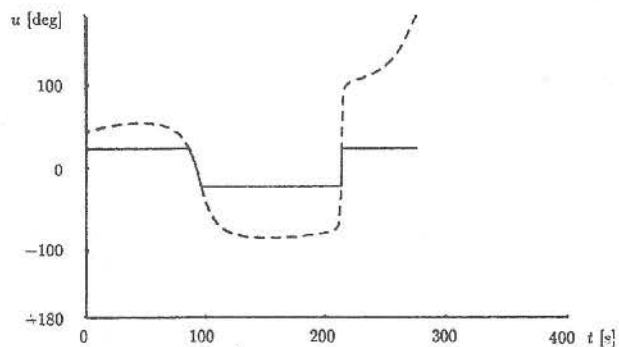


Figure 5. Control history for the Apollo re-entry; $u_{\max} = 23$ deg.

8.2. Maximum crossrange re-entry of a space-shuttle orbiter under a constraint of the skin temperature

For the numerical results of the space-shuttle re-entry problem of Section 3, it is mainly referred to Dickmanns and Pesch 1975 and Deuffhard et. al. 1976. The most recent results are given in Kugelmann and Pesch 1990B. The changes of the switching structure can be easily obtained when the control-unconstrained problem is solved first. For this case, the control history is given in Fig. 1 of Kugelmann and Pesch 1990B. By tightening the constraint, i.e., decreasing the value of ΔC_{LH} , up to four constrained subarcs appear. During the further course of the homotopy, ever the last two subarcs merge together until one long constrained subarc is finally left over. Compare Fig. 3 of Kugelmann and Pesch 1990B. The homotopy was stopped at $T \approx 924^\circ\text{C}$, where λ_V becomes

zero on the constrained subarc, i.e., the free control C_L^{free} is not defined beyond that point; see Eq. (27). For the results, see Fig. 4 of Kugelmann and Pesch 1990B. The heating constraint damps the oscillatory behavior of the trajectory; see Fig. 2 of Kugelmann and Pesch 1990B. Note that the problem is ill-conditioned with a condition number of about 10^{20} , if the so-called condensed multiple shooting version is used where the system of linear equations to be solved in each iteration step of the modified Newton method (78) is reduced to a smaller system with a coefficient matrix as given by the Eqs. (101). The condition number is of magnitude 10^8 only, if the large system with a coefficient matrix equivalent to (100) is solved. Notice that the application of the modified homotopy technique (81) accelerates the homotopy run considerably; see Deuffhard et. al. 1976. Figure 6 gives an impression of the re-entry trajectory for the control-unconstrained case. The heating constraint smoothes the trajectory. Oscillations only occur after having passed the boundary arc; see Fig. 2 of Kugelmann and Pesch 1990B.

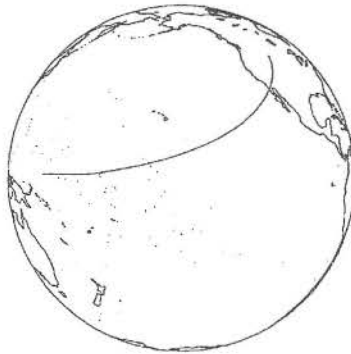


Figure 6. Re-entry trajectory for the Space-Shuttle re-entry; control-unconstrained case.

8.3. Minimum heating re-entry of an Apollo capsula under a constraint of the altitude

The introduction of the second-order state constraint has the same effect as the angle of attack constraint as described in Section 8.1 except that the final time does not decrease as much. Figures 7 and 8 show the histories of the altitude for $h_{\max} \approx 50.97$ km and $h_{\max} \approx 42.05$ km. The first trajectory has one touch point, the second one boundary arc and one touch point. Between these two values of h_{\max} , there are optimal solutions with two touch points; the first touch point splits to a boundary arc when the constraint is intensified. The changes from one switching structure to another can be detected with the help of graph-

ical output. Pay attention whether the component for the altitude as obtained from the solution of the boundary-value problem satisfies the constraint (40) for all t after the first dip into the atmosphere. The sign conditions (46) must be obeyed, too, and may help to single out nonoptimal solutions. Note that the deviation from the boundary h_{\max} between the boundary subarc and the touch point is approximately 30 m only. This problem was solved completely for the first time by Hiltmann 1983. The control histories of this problem can be found in Figs. 12–14 of Pesch 1989B.

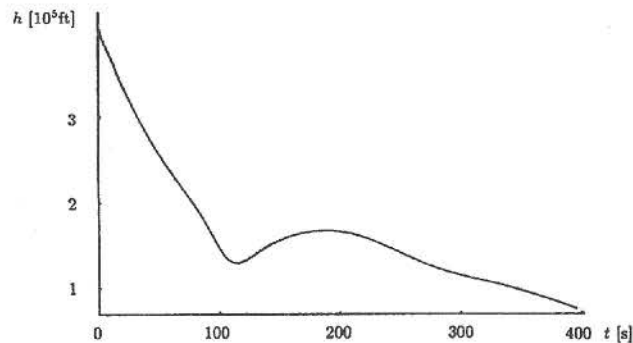


Figure 7. Altitude history for the Apollo re-entry; $h_{\max} \approx 50.97$ km.

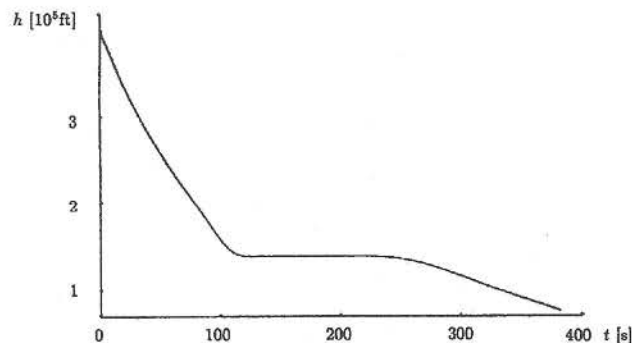


Figure 8. Altitude history for the Apollo re-entry; $h_{\max} \approx 42.05$ km.

8.4. Abort landing of a passenger aircraft under windshear conditions

Because the numerical results and the way of computing the solution are described in great detail in Bulirsch et. al. 1991B, we concentrate here on the treatment of singular subarcs only. Figures 9 and 10 show the switching function λ_α , see Eq. (59), for two distinct sets of boundary conditions at the very beginning of the homotopy for the state-unconstrained problem with the Bolza type functional (79) and $r = 3$. Figure 10 shows an optimal control history with a singular subarc. The transition from the completely nonsingular case as described by Fig. 9 to the problem of Fig. 10 with a singular subarc needs to determine which type of switching structure will be optimal. In this case, a solution with two additional bang-bang switching points, which also seems to be possible, could not be obtained. The multiple shooting method produces solutions contradicting Eq. (59) if the boundary-value problem is formulated for plane bang-bang structure.

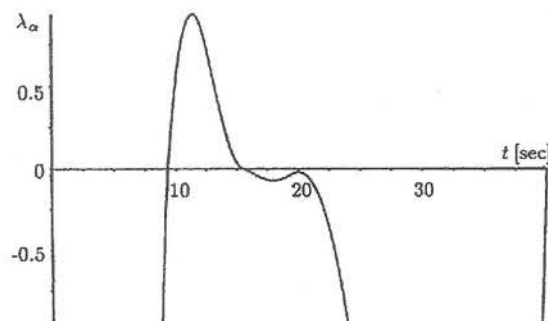


Figure 9. History of the switching function with plane bang-bang switching structure for the abort landing problem.

For the sake of completeness, Fig.11 shows the two trajectories in the vertical plane for the performance indices (55) (solid line) and (79) (dashed line) and the windprofile. See Pesch to appear for the detailed switching structure due to the third-order state constraint which is induced by the transformation (56) of the Chebyshev functional. Further results for different windshear intensities up to about 200 ft/sec for the difference between maximum tailwind and maximum headwind and for windshear profiles that also include upwind zones can be found in Berkman and Pesch to appear.

By the way, Bulirsch et. al. 1991A, 1991B may serve as a user's guide for solving sophisticated optimal control problems by multiple shooting. In particular, this windshear problem shows a lot of the features that make this optimal

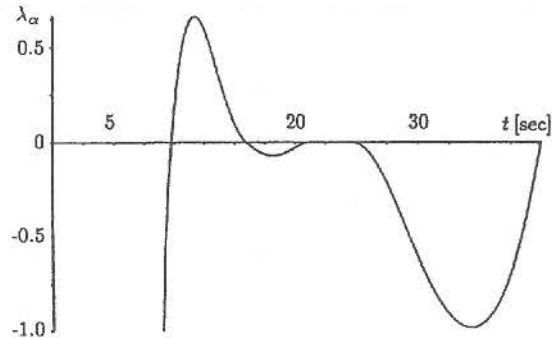


Figure 10. History of the switching function with one singular subarc for the abort landing problem.

control problem a tough one to solve. The papers provide a good illustration of how multiple shooting and homotopy techniques work in connection with optimal control problems involving multiple subarcs. Techniques are presented to detect, besides bang-bang subarcs, singular subarcs. In addition, the treatment of state constraints is explained in detail with emphasis on detection techniques for touch points and boundary subarcs. In particular, the modifications of the formulation of the multipoint boundary conditions are explained when changes of the switching structure appear during the homotopy runs. For the windhear problem, more than 15 such changes of the switching structure occurred, making that problem one of the most difficult ones ever solved by a numerical method. The complexity of optimal control problems can also be seen which at present can be solved by the multiple shooting method.

8.5. Maximum payload ascent of a two-stage-to-orbit space transporter system

The family of problems for the homotopy strategy to solve this problem consists of three major classes of subproblems; compare Section 7.2. First, solve the ascent problem in the plane of a great circle. At the time of stage separation the fuel of the first stage is assumed to be totally consumed; see Eqs. (71). Therefore, the following switching structure seems to be reasonable: $b = b_{I, \max}$ for $0 \leq t \leq t_{\text{stage}}$ and $b = b_{II, \max}$, $b = 0$, and $b = b_{II, \max}$ for $t_{\text{stage}} < t \leq t_f$. Second, make the transition to a three-dimensional coordinate system for a flight over a spherical Earth. Third, include Coriolis and centrifugal forces to obtain a model for a spherical rotating Earth.

For the first subproblem, convergence difficulties with the multiple shooting method arise because of the non-differentiability of the Hamiltonian at $t = t_f$ if the boundary condition (5d) is used; see Oberle 1976, 1977 for a similar problem.

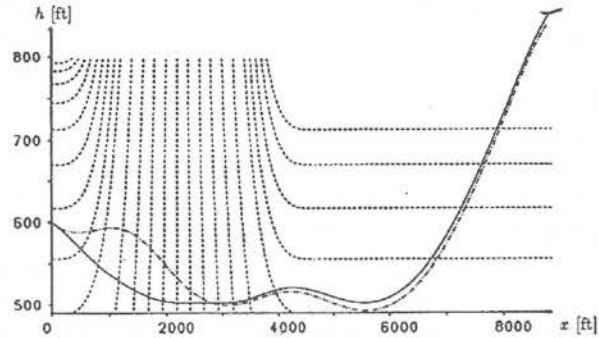


Figure 11. Abort landing of a passenger aircraft in a windshear; comparison between Bolza and Chebyshev functional.

This obstacle can be circumvent if the boundary condition (5d) is replaced by the equivalent condition $H(0) = 0$. Note that the problem is autonomous. Thus, $H \equiv \text{const}$ from which $H \equiv 0$ follows because of Eqs. (5d) and (67a).

For the numerical results of a more realistic model, see Bulirsch and Chudej 1992A and Chudej to appear. The trajectory of this upgraded model is taken from these references and given in Fig. 12.



Figure 12. Launch and stage separation of a Sänger-type space vehicle.

9. Neighboring extremals

If optimal solutions of processes which run down very fast, such as the optimal flight of space vehicles or aircrafts, are to be realized practically, one needs fast

numerical methods to compensate for disturbances occurring during the course of this process. This guarantees that optimality conditions and prescribed constraints are preserved. The required minimal computing time for the computation of an adjusted optimal control program cannot be met by the multiple shooting method if computers with conventional architectures are used. Despite the inherent parallel structure of the multiple shooting algorithm, it is today not yet thoroughly investigated whether computing times can be achieved by a parallel multiple shooting algorithm which are fast enough for on-line applications in the aerospace field. In this survey, we therefore go a different way.

In the following, we describe two numerical methods which are based, with respect to their theoretical part, on the theory of neighboring extremals and, with respect to their numerical part, on the multiple shooting method. A linearization of the necessary conditions of the disturbed optimal control problem around the optimal trajectory of the undisturbed problem leads to a linear multipoint boundary-value problem for the perturbations of the state and adjoint variables. This linear boundary-value problem can be solved very efficiently if appropriate information about the reference trajectory is pre-computed and stored in the onboard computer. Both methods allow the real-time computation of neighboring optimum feedback controls for control problems of a rather general class such as described in the foregoing sections. The two methods are described in detail in Pesch 1989A, 1989B and in Kugelmann and Pesch 1990A, 1990B, respectively. So, only the basic ideas are given here.

Optimal control problems are investigated which depend on a vector perturbation parameter. For the sake of simplicity, the considerations are restricted to problems with a perturbation parameter p entering the initial conditions

$$x(0) = \chi(p) \quad (82)$$

and/or the boundary conditions

$$\psi(x(t_f), t_f, p) = 0.$$

By including additional terms, the following linearization technique can be generalized for problems with perturbations in all other functions which are involved in the description of the underlying model. The disturbances will give rise to optimal solutions

$$x(t; p), \quad u(t; p), \quad t_f(p), \quad \lambda(t; p), \quad \dots \quad (83)$$

of the perturbed optimal control problem which can be shown to exist in a neighborhood of the optimal solution of the undisturbed problem, if certain regularity assumptions are satisfied. Moreover, these optimal solutions are continuously differentiable with respect to the perturbation parameter p near $p = 0$. For the class of problems, where this can be proven, see Maurer and Pesch to appear. Because of the continuous differentiability with respect to p , we may define the

so-called variations

$$\delta x(t) := \frac{\partial x}{\partial p}(t; 0) p, \quad \delta \lambda(t) := \frac{\partial \lambda}{\partial p}(t; 0) p, \quad (84a)$$

$$\delta u(t) := \frac{\partial u}{\partial p}(t; 0) p, \quad \delta \mu(t) := \frac{\partial \mu}{\partial p}(t; 0) p, \quad (84b)$$

and the differentials

$$dt_f := \frac{dt_f}{dp}(0) p, \quad d\nu := \frac{d\nu}{dp}(0) p, \quad (84c)$$

$$dx(t_{f_0}) := \delta x(t_{f_0}) + \dot{x}_0(t_{f_0}) dt_f, \quad d\lambda(t_{f_0}) := \delta \lambda(t_{f_0}) + \dot{\lambda}_0(t_{f_0}) dt_f \quad (84d)$$

where $x_0 = x(t; 0)$, $u_0 = u(t; 0)$, $\lambda_0 = \lambda(t; 0)$ and $t_{f_0} = t_f(0)$ denote an optimal solution of the undisturbed problem. These variations have now to be computed to obtain a first-order optimal solution of the disturbed problem, e.g., by

$$x(t; p) \doteq x_0 + \delta x(t), \quad (85a)$$

$$u(t; p) \doteq u_0 + \delta u(t), \quad (85b)$$

$$t_f(p) \doteq t_{f_0} + dt_f. \quad (85c)$$

Therefore, the result obtained in this way is called a neighboring extremal. For additional references, see Pesch 1989A.

For the sake of simplicity and brevity, we consider optimal control problems with one mixed constraint ($l = 1$), where $C_u \neq 0$, and a scalar control variable ($k = 1$). The boundary conditions are assumed to be disturbed,

$$\delta x_0 = \delta x(t_0) \doteq x(t_0; p) - x_0(t_0) \quad \text{for } t_0 \in [0, t_f[, \quad (86a)$$

$$d\psi = \psi(x(t_f(p); p), t_f(p)). \quad (86b)$$

The perturbation vector p is assumed to be given at the time of measurement t_0 ,

$$p := \begin{pmatrix} \delta x_0 \\ d\psi \end{pmatrix} \in \mathbb{R}^{n+q}. \quad (87)$$

A linearization of the Eqs. (2a), (5a), (9a), (2b), (2c), (5c), and (5d) with the Hamiltonian (18) around the optimal solution of the undisturbed problem gives

$$\delta \dot{x} = f_x \delta x + f_u \delta u, \quad (88a)$$

$$\delta \dot{\lambda} = -H_{xx} \delta x - H_{xu} \delta u - f_x^\top \delta \lambda - C_x^\top \delta \mu, \quad (88b)$$

$$0 = H_{ux} \delta x + H_{uu} \delta u + f_u^\top \delta \lambda + C_u \delta \mu, \quad (88c)$$

$$\delta x(t_0) = \delta x_0, \quad (88d)$$

$$d\psi = (\psi_x dx + \psi_t dt_f) |_{t_{f_0}}, \quad (88e)$$

$$d\lambda(t_f) = (\Phi_{xx} dx + \psi_x^\top d\nu + \Phi_{xt}^\top dt_f) |_{t_{f_0}}, \quad (88f)$$

$$0 = \left((\Phi_{xt} - \dot{\lambda}_0^\top) dx + \dot{x}_0^\top d\lambda + \Phi_{tt} dt_f + \psi_t^\top d\nu \right) |_{t_{f_0}}. \quad (88g)$$

All vector- or matrix-valued functions are to be evaluated along the optimal solution of the nominal problem, e.g.,

$$H_{xu} := \frac{\partial}{\partial u} H_x^\top = H_{xu}(x_0, u_0, \lambda_0, \mu_0).$$

In the last equation, the vanishing terms $H_u du$ (because of Eq. (9a)) and $C d\mu$ (either $C = 0$ or $d\mu = 0$ because of Eq. (19)) are omitted.

For the further investigation, we assume that the Hamiltonian is regular and that the strong Legendre-Clebsch condition (9b) is valid on unconstrained subarcs. As in the previous sections, we have to distinguish between unconstrained and constrained subarcs. In addition, we must take into account that the control laws being active at the time of correction might be different for the nominal and the actual trajectory, particularly in the neighborhood of the nominal switching points. Here, we consider the two simpler cases only where the same behavior of the control variable is present along the undisturbed and disturbed trajectory. For the other cases, see Pesch 1989A.

1st Case: $C(x(t;p), u(t;p)) < 0$ and $C(x_0(t), u_0(t)) < 0$.

Since $\mu(t;p) = 0$ and also $\mu_0(t) = 0$ hold, it follows $\delta\mu(t) = 0$. From Eq. (88c) and by applying the Implicit Function Theorem to Eq. (9a), one obtains

$$\delta u = -H_{uu}^{-1} \cdot (H_{ux} \delta x + f_u^\top \delta \lambda) = u_x \delta x + u_\lambda \delta \lambda. \quad (89)$$

Substituting Eq. (89) into Eqs. (88a) and (88b) yields a homogeneous system of differential equations for the variations δx and $\delta \lambda$,

$$\begin{pmatrix} \delta \dot{x} \\ \delta \dot{\lambda} \end{pmatrix} = \begin{pmatrix} A(t) & B(t) \\ \tilde{B}(t) & -A^\top(t) \end{pmatrix} \cdot \begin{pmatrix} \delta x \\ \delta \lambda \end{pmatrix} \quad (90)$$

where

$$A(t) = f_x - f_u H_{uu}^{-1} H_{ux} = f_x + f_u u_x = \frac{df}{dx},$$

$$B(t) = -f_u H_{uu}^{-1} f_u^\top = f_u u_\lambda = \frac{df}{d\lambda},$$

$$\tilde{B}(t) = -H_{xx} + H_{xu} H_{uu}^{-1} H_{ux} = -H_{xx} - H_{xu} u_x = \frac{dg}{dx},$$

$$B(t) = B^\top(t), \quad \tilde{B}(t) = \tilde{B}^\top(t), \quad \frac{dg}{d\lambda} = - \left(\frac{df}{dx} \right)^\top = -A^\top(t),$$

with

$$g(x, \lambda) := -H_x^\top(x, u(x, \lambda), \lambda, \mu(x, \lambda)).$$

2nd Case: $C(x(t; p), u(t; p)) = 0$ and $C(x_0(t), u_0(t)) = 0$.

Under the assumption $C_u \neq 0$, we obtain by linearizing $C(x(t; p), u(t; p)) = 0$,

$$\delta u = -C_u^{-1} C_x \delta x = u_x \delta x, \quad (91)$$

and Eq. (88c) yields

$$\delta \mu = -C_u^{-1} \cdot (H_{ux} \delta x + H_{uu} \delta u + f_u^\top \delta \lambda). \quad (92a)$$

Applying the Implicit Function Theorem on Eq. (9a) with (18), this equation can be written as

$$\delta \mu = \mu_x \delta x + \mu_u \delta u + \mu_\lambda \delta \lambda \quad (92b)$$

where

$$\mu_x = -C_u^{-1} H_{ux}, \quad \mu_u = -C_u^{-1} H_{uu}, \quad \mu_\lambda = -C_u^{-1} f_u^\top$$

Substituting Eqs. (91) and (92) into (88a) and (88b) leads to

$$\begin{pmatrix} \delta \dot{x} \\ \delta \dot{\lambda} \end{pmatrix} = \begin{pmatrix} A(t) & 0 \\ \tilde{B}(t) & -A^\top(t) \end{pmatrix} \cdot \begin{pmatrix} \delta x \\ \delta \lambda \end{pmatrix} \quad (93)$$

where

$$\begin{aligned} A(t) &= f_x - f_u C_u^{-1} C_x = f_x + f_u u_x = \frac{df}{dx}, \\ \tilde{B}(t) &= -H_{xx} + H_{xu} C_u^{-1} C_x + C_x^\top C_u^{-1} \cdot (H_{ux} - H_{uu} C_u^{-1} C_x), \\ &= \frac{dg}{dx} = g_x + g_u u_x + g_\mu \cdot (\mu_x + \mu_u u_x). \end{aligned}$$

In both of these cases, the arguments of the coefficient functions are just the nominal extremal x_0, u_0, λ_0 and μ_0 .

Note that there may also exist an explicit nonlinear feedback law on constrained subarcs; see Eq. (21).

The gaps between nominal and actual switching points are covered by the two cases $C(x(t; p), u(t; p)) < 0$ and $C(x_0(t), u_0(t)) = 0$, and $C(x(t; p), u(t; p)) = 0$ and $C(x_0(t), u_0(t)) < 0$, respectively. For these cases, the linearization must be done so that the system of linear differential equations for the variations remains homogeneous. See Pesch 1989A for details. This property is of utmost importance for the efficiency of the guidance schemes developed in Section 10.

In a similar way, the interior point constraints and the jump conditions are linearized. In addition, linear relations are obtained from the switching conditions to approximate the displacements of the switching points. In summary, all these linearized necessary conditions lead to a linear multipoint boundary-value problem with homogeneous differential equations, linear multipoint boundary conditions, and linear jump conditions, that is especially well-suited for real-time computations. See Pesch 1989A.

10. On-line computation of optimal trajectories by neighboring optimum feedback guidance schemes

10.1. Multiple shooting for linear multipoint boundary-value problems

The linearized necessary conditions of Section 9 lead to a linear multipoint boundary-value problem of the following form,

$$\dot{y}(t) = T(t)y(t) \quad \text{for } \tau_j \leq t < \tau_{j+1}, \quad j = 1, \dots, m-1, \quad (94a)$$

$$A y(\tau_1) + \sum_{j=2}^{m-1} A_{s_j} y(\tau_j^-) + B y(\tau_m) - c(p) = 0, \quad (94b)$$

$$y(\tau_j^+) = R_{s_j} y(\tau_j^-) \quad \text{for } j = 2, \dots, m-1, \quad (94c)$$

$$0 = \tau_1 < \tau_2 < \dots < \tau_m = t_f \quad (94d)$$

where $T: [0, t_f] \rightarrow \mathbb{R}^{\bar{N}, \bar{N}}$ is piecewise continuous, A , A_{s_j} , B and R_{s_j} are \bar{N} by \bar{N} -matrices, and c is an \bar{N} -vector. Here, $y^\top := (\delta x^\top, \delta \lambda^\top, d\pi_1, \dots, d\pi_Q)$ contains the variations δx and $\delta \lambda$ of the state vector and the adjoint multiplier, respectively, from which the variation δu of the control vector can be computed by a linear relationship of the form,

$$\delta u(t) = u_x(x_0(t), \lambda_0(t)) \delta x(t) + u_\lambda(x_0(t), \lambda_0(t)) \delta \lambda(t). \quad (95)$$

Note that there holds $u_\lambda = 0$ on state-constrained subarcs. The variations $d\pi_k$ are associated with the multipliers for the interior point conditions. These variations as well as the differentials $d\tau_j$ of the nominal switching points τ_j , $j = 2, \dots, m-1$, are needed to approximate the optimal solution of the perturbed optimal control problem to the first order. The actual switching points are obtained analogously to Eqs. (85) by additional linear relations for the displacements $d\tau_j$,

$$d\tau_j = -\dot{W}^{-1}(W_x, W_\lambda) \begin{pmatrix} \delta x(\tau_j) \\ \delta \lambda(\tau_j) \end{pmatrix} \quad (96)$$

where $W(x(\tau_j), \lambda(\tau_j)) = 0$ denotes the switching condition associated with the switching point τ_j . The subscript 0 for the characterization of the nominal switching points is omitted here. See Pesch 1989A, 1989B for details. Finally, it should be mentioned that the vector perturbation parameter p enters only the vector c in the above linear boundary-value problem (94). This also is of utmost importance for the efficiency of the guidance methods developed in the following subsections.

The solution of this boundary-value problem can be reduced to the solution of a series of initial-value problems as in the multiple shooting method of Section 7. We start again on the basis of a subdivision of the interval $[0, t_f]$, which

can be assumed to coincide with the partition (94d) without loss of generality. Take simply $R_{s_j} = I$ and $A_{s_j} = 0$ to include additional multiple shooting nodes. The following initial-value problems are now to be solved,

$$\dot{y} = Ty \quad \text{for } \tau_j \leq t < \tau_{j+1}, \quad j = 1, \dots, m-1, \quad (97a)$$

$$y(\tau_j; s_j) = s_j \quad \text{with } s_j \in \mathbb{R}^{\bar{N}}. \quad (97b)$$

The unique solutions

$$y(t; s_j) = Y(t; \tau_j) s_j \quad \text{for } \tau_j \leq t < \tau_{j+1} \quad (98)$$

can be given in terms of the transition matrices $Y(t; \tau_j)$, $j = 1, \dots, m-1$, defined by the matrix initial-value problems

$$\frac{\partial}{\partial t} Y(t; \tau_j) = T Y(t; \tau_j), \quad (99a)$$

$$Y(\tau_j; \tau_j) = I_{\bar{N}}. \quad (99b)$$

Here, $I_{\bar{N}}$ denotes the identity matrix of dimension \bar{N} . The unknown vectors s_j , denoting the right-hand-side values of the variations at discontinuities, are to be determined so that the solutions (98) satisfy the multipoint boundary conditions (94b) and the jump conditions (94c). This leads to the following system of $\bar{N}(m-1)$ linear equations,

$$\begin{pmatrix} R_{s_2} Y_1 & -I & O & O & \dots & O \\ O & R_{s_3} Y_2 & -I & O & \dots & O \\ O & O & R_{s_4} Y_3 & -I & & O \\ \vdots & & & \ddots & \ddots & \vdots \\ O & & & & & O \\ A + A_{s_2} Y_1 & A_{s_3} Y_2 & \dots & O & R_{s_{m-1}} Y_{m-2} & -I \\ & & \dots & \dots & A_{s_{m-1}} Y_{m-2} & B Y_{m-1} \end{pmatrix} \begin{pmatrix} s_1 \\ s_2 \\ s_3 \\ \vdots \\ s_{m-3} \\ s_{m-2} \\ s_{m-1} \end{pmatrix} = \begin{pmatrix} 0 \\ 0 \\ 0 \\ \vdots \\ 0 \\ 0 \\ c \end{pmatrix} \quad (100)$$

where

$$Y_j := Y(\tau_{j+1}; \tau_j).$$

By an appropriate elimination, the number of equations in (100) can be reduced to \bar{N} ,

$$E s_1 = c \quad (101a)$$

where

$$E = \sum_{j=1}^m A_{s_j} \prod_{i=1}^{j-1} Y_{j-i} R_{s_i} \quad (101b)$$

and

$$A_{s_1} := A, \quad A_{s_m} := B, \quad R_{s_1} := I. \quad (101c)$$

Moreover, we have, for $j = 2, \dots, m$, the recursion

$$s_j = R_{s_j} Y_{j-1} s_{j-1}, \quad (102a)$$

$$R_{s_m} := I. \quad (102b)$$

Because of the special block structure of the matrices T and A_{s_i} of the boundary-value problem (94), the coefficient matrix E has a special block structure, too,

$$E = \begin{pmatrix} I & O \\ E_1 & E_2 \end{pmatrix}.$$

For details, see Pesch 1989B. Therefore, the number of equations in (101a) can be reduced once more. According to the partition of the vector y , one obtains, introducing the subpartition,

$$y = (y_A^\top, y_B^\top)^\top, \quad y_A = \delta x, \quad y_B = (\delta \lambda^\top, d\pi_1, \dots, d\pi_Q)^\top, \quad (103a)$$

$$c = (c_A^\top, c_B^\top)^\top, \quad s_1 = (s_{1A}^\top, s_{1B}^\top)^\top, \quad (103b)$$

the following system of linear equations,

$$E_2 s_{1B} = c_B - E_1 c_A, \quad s_{1A} = c_A. \quad (104)$$

Generally, this system has considerably fewer equations than (100); but for very sensitive problems, the elimination process leading to (101) may change the condition number for the worse, since the elimination is a Gauss algorithm performed blockwise with fixed pivoting. For moderately conditioned problems, however, Eq. (101) is preferable to (100) for on-line computations because of its lower computation and storage requirements. Compare also the remarks in Section 8.2.

10.2. The neighboring optimum feedback guidance scheme

In summary, we obtain from Eq. (104) a first guidance method where the main computational effort for computing the neighboring optimal control vector can be carried through before starting the process, e.g., before the take-off of a space vehicle. The main part of the computation to be performed before the process is started is the approximation of the transition matrices Y_j .

If we solve Eq. (104) for s_{1B} and substitute the result in the linear formula (95) for δu , we obtain a continuous neighboring optimum feedback law of the form

$$\delta u(t_0) = \Lambda_1(t_0) \delta x_0 + \Lambda_2(t_0) d\psi \quad (105)$$

where the so-called gain matrices Λ_1 and Λ_2 can be precomputed. Here t_0 denotes the correction time, δx_0 the measured deviation from the reference path

at this time, and $d\psi$ the change in the terminal conditions. For more details, see Kugelmann and Pesch 1990A, 1990B. The amount of computation during the process, namely the matrix-times-vector operations, is negligible. This feedback scheme can be described by the diagram in Fig. 13.

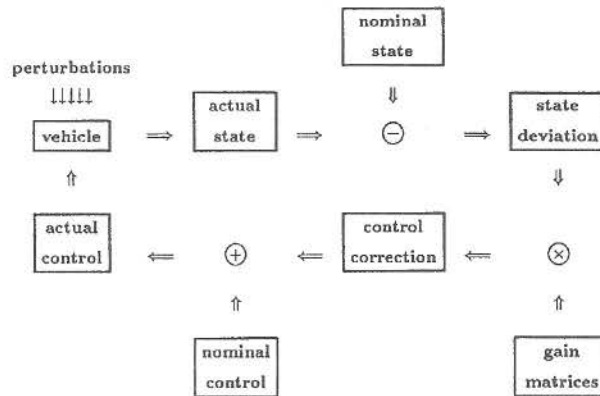


Figure 13. Chartflow of the neighboring optimum feedback guidance scheme.

If we assess the pros and cons of this method, we see that, in spite of the advantageous low onboard computations, the method shows some disadvantages. For example, the method will fail if measurement data are absent for a while. Moreover, a precheck of the constraints and a reliable precomputation of the switching points, before feeding back the adjusted control, are impossible. Even if we would use the recurrence (102a), the results would be unsatisfactory since the use of transition matrices if integrated over longer intervals leads to an exponential growth of the linearization error. These disadvantages can be avoided by the following surer but also costlier method.

10.3. The repeated correction guidance scheme

Because of the many technical details of the improved method, which is called repeated correction method, we describe here the idea of the method only. For the details, it is again referred to Pesch 1989A, 1989B.

The evaluation of the neighboring optimum feedback scheme (105) or, alternatively, the solution of the linear system (104) is incorporated into the numerical integration of the equations of motion with the control variables approximated by spline functions for example. A single integration of the equations of motion then yields an approximation of the actual trajectory for the entire remaining flight time interval. This approximation also includes the approximation of all switching points. It is obvious that this full information can, in

addition, be used to check the observance of all constraints imposed on the problem. By this approach, a verified feedback scheme is available which is not so dependent on a continuous flow of the measurement data as the linear feedback scheme of the previous subsection. Note that the repeated correction, either at many sample points or continuously, reduces the influence of the linearization error introduced by the theory of Section 9. This indeed is just the self-correcting property of Newton's method. By the linearization and the subsequent application of the multiple shooting discretization to the linear boundary-value problem, we end up with the same system of linear equations that is obtained in the multiple shooting iteration when applied to the disturbed problem with the undisturbed solution as initial estimate. This error damping property also holds for the method of Section 10.2 if applied synchronously with the flow of data. With this respect, both methods are equivalent. This leads to controllability regions of about the same size for both methods. The controllability region of a guidance method describes the set of all deviations from the reference path which can be successfully compensated during the course of the process. Because the linearization step and the discretization step can be interpreted as commutative operators, the controllability regions of both guidance methods are also equivalent to the domain of convergence of the undamped Newton iteration, i.e., take $\rho^{(i)} = 1$ for all i in Eq. (78); see Pesch 1990B. Therefore, the computation of the domain of convergence of the multiple shooting method with the standard Newton method provides a quick test for controllability; see Kugelmann and Pesch 1991.

One cannot expect the onboard computing time for this more sophisticated method to be negligible compared with the remaining flight time. Therefore, we first integrate the equations of motion in real-time over a small interval $[t_0 - \Delta t_0, t_0]$, $\Delta t_0 > 0$, by using the measured actual state vector at $t_0 - \Delta t_0$ as the initial value. The control vector is chosen either as the actual control computed last or, if not available, as the nominal control. The actual control history due to this precomputed future deviation from the nominal trajectory at time t_0 is then computed. During the onboard computation, the vehicle is assumed to fly to this so precomputed state at t_0 so that the actual control can be started in due time after completion of the computation. Here Δt_0 is selected as an upper bound for the onboard computing time needed. This feedback scheme can be described by the diagram of Fig. 14.

Finally, it should be mentioned that the parallel structure of the multiple shooting method can still be preserved, if the linear system (100) is taken for the repeated correction algorithm which, moreover, has the better numerical stability properties. Then, the numerical integration and the check of the constraints can be split up into different segments and, therefore, can be carried through on different processors. The linearization error, however, cannot be smoothed as well as by the serial version of the repeated correction method; for the discussion of this effect, see Kugelmann and Pesch 1990C.

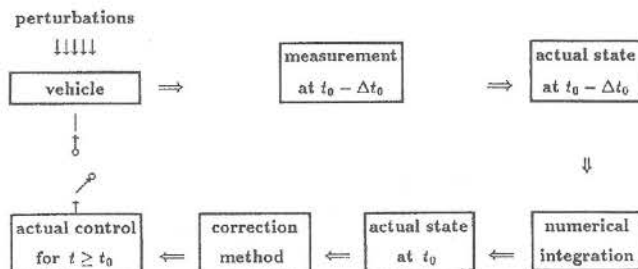


Figure 14. Chartflow of the repeated correction guidance scheme.

11. Numerical results II

For the optimal control problems considered in the Sections 2–4 and 6, investigations have been made concerning the controllability of the optimal trajectories. In Pesch 1979, 1989B, 1990A, the Apollo re-entry problems are discussed. Investigations for the Space-Shuttle re-entry problem can be found in Pesch 1980 and in Kugelmann and Pesch 1990B and for the Sanger ascent in Kugelmann and Pesch 1991. Here, results are presented only for the Space-Shuttle re-entry problem. Figure 15 shows some trajectories around the reference flight path for simulated deviations from the nominal altitude, which have been computed by means of the neighboring optimum guidance scheme of Section 10.2. The cross section through the controllability tube around the nominal trajectory in the direction of the altitude abscissa is also indicated.

The numerical results for the cross-range maximization problem of a space-shuttle glider under a radiative heating constraint, as obtained and discussed in Kugelmann and Pesch 1990B, show that, even for that extremely sensitive problem, the domain of controllability is large enough for practical applications. The domain of controllability for terminal perturbations is considerably smaller, since it may be inherent for all feedback schemes that use some information from a reference trajectory.

Together with the more costly repeated correction method, two variants of a multiple shooting based guidance method are available which are numerically stable and nearly optimal. These can be applied either to guidance problems requiring extremely fast corrections — the observance of the constraints can only be guaranteed to the first order in this case — or to problems that allow more expensive computations — in which case all constraints are checked and even a limited absence of measurement data is not disastrous.

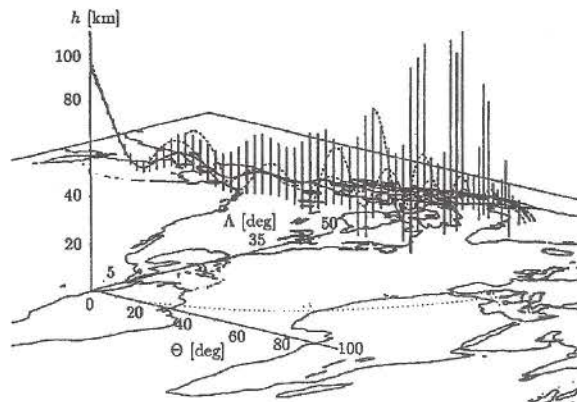


Figure 15. Neighboring optimal trajectories around the optimal reference trajectory for the Space-Shuttle re-entry.

12. Conclusions and outlook

The trend in the numerical treatment of optimal control problems in aerospace engineering points towards problems of increasing complexity in order to approximate reality as closely as possible. These problems lead rather to an increasing number of constraints than to an increasing number of unknowns involved in the problems. Thus, engineers and mathematicians who are involved in the design and development of future aerospace enterprises have a strong demand for reliable and efficient software that can handle optimal control problems with different types of constraints. Despite the fact that a direct method, such as a direct collocation method, may be easier to apply, since only a little knowledge of optimal control theory is required, the indirect multiple shooting method has advantages with respect to reliability, precision, and getting insight into the structure of the solution and its optimality. Moreover, the multiple shooting method is especially appropriate for an implementation on parallel computers; see Kiehl 1989.

Concerning the off-line computation of optimal trajectories of complex control problems, both theory and software have reached a high standard. The limit of problems which today can be solved by the multiple shooting method in the field of aerospace applications can be seen, for example, from the investigations of ion-driven gravity-assisted missions to asteroids like Flora and Vesta, see Bulirsch and Callies 1991A, 1991B, and to outer planets like Neptune, see Callies to appear. The multiple rendezvous mission to asteroids, for example, is modelled by an optimal control problem subject to several control and state variable inequality constraints, several interior point constraints and parameter

constraints. The fully optimized trajectory including a Moon swing-by and spiraling down to and up from low asteroid orbits exhibits more than 50 switching points. For complex missions like this, the outstanding accuracy provided by the multiple shooting method is no longer an unnecessary by-product of an over-precise or overdeveloped method, but of vital and decisive importance for the mission planning. The high accuracy renders possible the computation of the optimal trajectory at all.

For the optimal control of industrial robots, the equations of motion themselves are very complicated and, in general, established by means of appropriate software. The adjoint differential equations can then be obtained via symbolic differentiation. Minimum-time and minimum-energy trajectories for an industrial robot of three degrees of freedom are investigated in Pesch et. al. to appear and von Stryk and Schlemmer to appear. See also Pesch to appear. The numerical results have been obtained both by means of a direct collocation and by means of a multiple shooting method. Because of the high complexity of the adjoint variables (more than 3,000 FORTRAN statements for the right-hand sides of the differential equations), the direct collocation method is preferable to any indirect method for this kind of problems.

Contrary to the off-line computation of optimal trajectories, both the theoretical and the numerical basis for the on-line computation of optimal trajectories are not as well-developed when optimal control problems of a rather general class, as covered in this paper, are considered. The theoretical foundation which is related to second-order sufficient optimality conditions, see Maurer and Pesch to appear, is not yet well understood if state inequality constraints are taken into account, although their numerical treatment turns out to be a routine work today. Despite the missing mathematical justification, the guidance schemes based on the theory of neighboring extremals show their applicability for the real-time computation of optimal trajectories for control problems which include control and/or state variable inequality constraints; see Pesch 1989A, 1989B and Kugelmann and Pesch 1990A, 1990B. Open questions are concerned with problems having singular subarcs, and also the numerical realization of a neighboring optimum guidance scheme which can compensate disturbances of system parameters, e.g., air density fluctuations, is still pending.

A new approach for problems of the latter type is via differential game theory where the unknown air density fluctuations are modelled as the controls of an antagonistic player in a two-person zero-sum differential game; see Breitner and Pesch to appear. By this approach, not only the worst case can be studied but optimal strategies can be computed for density fluctuations within limits that are known from long time measurements; see Breitner to appear and Fig. 16.

In the near future, methods designed for the off-line computation of optimal trajectories will be able to compete because of the rapidly increasing speed of computation due to parallel computers if they are available for onboard computers on spacecraft, too. Parallelized versions of indirect or direct multiple shooting seem to be the most promising techniques because of the inherent

parallel structure of the multiple shooting algorithm.

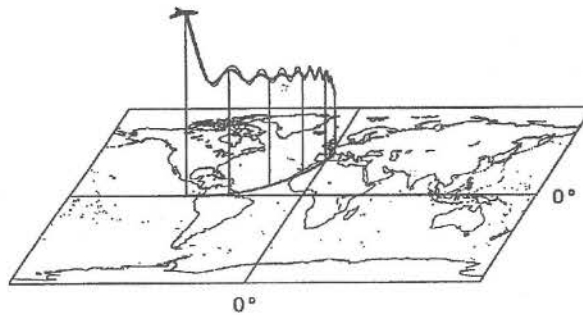


Figure 16. Re-entry of a shuttle under uncertain air density disturbances: Optimal control solution (thin line) and differential game solution (thick line) for the control unconstrained case of Section 3.

References

- BERKMANN P. AND PESCH H.J. Abort Landing under Different Windshear Conditions, to appear.
- BREAKWELL J.V., SPEYER J.L. AND BRYSON A.E. (1963) Optimization and Control of Nonlinear Systems Using the Second Variation, *SIAM Journal on Control* 1, pp. 193-223.
- BREITNER M. H. Construction of the Optimal Feedback Controller for Constrained Optimal Control Problems with Unknown Disturbances, *Proceedings of the 9th IFAC Workshop of Control Applications of Optimization*, Edited by R. Bulirsch and D. Kraft, International Series of Numerical Mathematics, Basel: Birkhäuser, to appear.
- BREITNER M. H. AND PESCH H. J. Re-entry Trajectory Optimization Under Atmospheric Uncertainty as a Differential Game, *Advances in Dynamic Games and Applications*, Edited by T. Başar et al. Annals of the ISDG, Vol. 1, Basel: Birkhäuser, to appear.
- BRYSON A. E. AND HO Y. C. (1987) Applied Optimal Control, Washington, D.C.: Hemisphere.
- BULIRSCH R. (1971) Die Mehrzielmethode zur numerischen Lösung von nicht-linearen Randwertproblemen und Aufgaben der optimalen Steuerung, Report of the Carl-Cranz Gesellschaft, Oberpfaffenhofen: Carl-Cranz Gesellschaft.
- BULIRSCH R. AND CALLIES R. (1991A) Optimal Trajectories for an Ion Driven Spacecraft from Earth to the Planetoid Vesta, Proceedings of

- the AIAA Guidance, Navigation and Control Conference, New Orleans, Louisiana, 1991, *AIAA Paper* 91-2683.
- BULIRSCH R. AND CALLIES R. (1991B) Optimal Trajectories for a Multiple Rendezvous Mission to Asteroids, 42nd International Astronautical Congress, Montreal, Canada, 1991, *IAF-Paper* IAF-91-342.
- BULIRSCH R. AND CHUDEJ K. (1991) Ascent Optimization of an Airbreathing Space Vehicle, Proceedings of the AIAA Guidance, Navigation and Control Conference, New Orleans, Louisiana, 1991, *AIAA Paper* 91-2656.
- BULIRSCH R. AND CHUDEJ K. (1992A) Staging and Ascent Optimization of a Dual-Stage Space Transporter, *Zeitschrift für Flugwissenschaften und Weltraumforschung* **16**, pp. 143-151.
- BULIRSCH R. AND CHUDEJ K. (1992B) Guidance and Trajectory Optimization under State Constraints, *Preprint of the 12th IFAC Symposium on Automatic Control in Aerospace — Aerospace Control 1992*, Edited by D. B. DeBra and E. Gottzein, Düsseldorf: VDI/VDE-GMA, pp. 553-538.
- BULIRSCH R., MONTRONE F. AND PESCH H.J. (1991A) Abort Landing in the Presence of a Windshear as a Minimax Optimal Control Problem, Part 1: Necessary Conditions, *Journal of Optimization Theory and Applications* **70**, pp. 1-23.
- BULIRSCH R., MONTRONE F. AND PESCH H.J. (1991B) Abort Landing in the Presence of a Windshear as a Minimax Optimal Control Problem, Part 2: Multiple Shooting and Homotopy, *Journal of Optimization Theory and Applications* **70**, pp. 223-254.
- BULIRSCH R., NERZ E., PESCH H.J. AND VON STRYK O. Combining Direct and Indirect Methods in Optimal Control: Range Maximization of a Hang Glider, *Optimal Control*, Proceedings of the Conference in Optimal Control and Variational Calculus, Oberwolfach, 1991, Edited by R. Bulirsch et. al., Basel: Birkhäuser, to appear.
- CALLIES R. Optimal Design of a Mission to Neptune, *Optimal Control*, Proceedings of the Conference in Optimal Control and Variational Calculus, Oberwolfach, 1991, Edited by R. Bulirsch et. al., Basel: Birkhäuser, to appear.
- CHUDEJ K. Optimization of the Stage Separation and the Flight of a Future Launch Vehicle, *Proceedings of the 16th IFIP Conference on System Modelling and Optimization*, Compiègne, 1993, Lecture Notes in Control and Information Science, Berlin: Springer, to appear.
- DEUFLHARD P. (1974) A Modified Newton Method for the Solution of Ill-conditioned Systems of Nonlinear Equations with Application to Multiple Shooting, *Numerische Mathematik* **22**, pp. 289-315.
- DEUFLHARD P. (1975) A Relaxation Strategy for the Modified Newton Method, *Optimization and Optimal Control, Lecture Notes in Mathematics* **477**, Edited by R. Bulirsch et. al., Berlin: Springer, pp. 59-73.
- DEUFLHARD P., PESCH H.J. AND RENTROP P. (1976) A Modified Continu-

- ation Method for the Numerical Solution of Nonlinear Two-Point Boundary Value Problems by Shooting Techniques, *Numerische Mathematik* **26**, pp. 327-343.
- DICKMANN E.D. AND PESCH H.J. (1975) Influence of a Reradiative Heating Constraint on Lifting Entry Trajectories for Maximum Lateral Range, *Proceedings of the 11th International Symposium on Space Technology and Science*, Tokyo, Japan, pp. 241-246.
- HILTMANN P. (1983) Numerische Behandlung optimaler Steuerprozesse mit Zustandsbeschränkungen mittels der Mehrzielmethode, Diploma Thesis, Department of Mathematics, Munich University of Technology, Munich.
- JACOBSON D.H., LELE M.M. AND SPEYER J.L. (1971) New Necessary Conditions of Optimality for Control Problems with State-Variable Inequality Constraints, *Journal of Mathematical Analysis and Application* **35**, pp. 255-284.
- KELLEY H.J., KOPP R.E. AND MOYER H.G. (1967) Singular Extremals, *Topics in Optimization*, Edited by G. Leitmann, New York: Academic Press, pp. 63-101.
- KIEHL M (1989) Vectorizing the Multiple-Shooting Method for the Solution of Boundary-Value Problems and Optimal Control Problems, *Proceedings of the 2nd International Conference on Vector and Parallel Computing Issues in Applied Research and Development*, Tromsø, 1988, Edited by J. Dongarra et. al., London: Ellis Horwood, pp. 179-188.
- KUGELMANN B. AND PESCH H.J. (1990A) New General Guidance Method in Constrained Optimal Control, Part 1: Numerical Method, *Journal of Optimization Theory and Applications* **67**, pp. 421-435.
- KUGELMANN B. AND PESCH H.J. (1990B) New General Guidance Method in Constrained Optimal Control, Part 2: Application to Space Shuttle Guidance, *Journal of Optimization Theory and Applications* **67**, pp. 437-446.
- KUGELMANN B. AND PESCH H.J. (1990C) Serielle und parallele Algorithmen zur Korrektur optimaler Flugbahnen in Echtzeit-Rechnung, Jahrestagung der Deutschen Gesellschaft für Luft- und Raumfahrt, Friedrichshafen, *DGLR-Jahrbuch 1990* **1**, pp. 233-241.
- KUGELMANN B. AND PESCH H.J. (1991) Real-Time Computation of Feedback Controls with Applications in Aerospace Engineering, Proceedings of the AIAA Guidance, Navigation and Control Conference, New Orleans, Louisiana, 1991, *AIAA Paper* 91-2658.
- MAURER H. (1976) Optimale Steuerprozesse mit Zustandsbeschränkungen, Habilitationsschrift, University of Würzburg, Würzburg.
- MAURER H. AND PESCH H.J. Solution Differentiability for Nonlinear Parametric Control Problems, *SIAM Journal on Control and Optimization*, to appear.
- MAURER H. AND PESCH H.J. Solution Differentiability for Parametric Nonlinear Control Problems with Inequality Constraints, *Proceedings of the 16th IFIP Conference on System Modelling and Optimization*, Compiègne,

- 1993, Lecture Notes in Control and Information Science, Berlin: Springer, to appear.
- MCDANELL J.P. AND POWERS W.F. (1971) Necessary Conditions for Joining Optimal Singular and Nonsingular Subarcs, *SIAM Journal on Control* **9**, pp. 161-173.
- MIELE A., WANG T. AND MELVIN W.W. (1987) Optimal Abort Landing Trajectories in the Presence of Windshear, *Journal of Optimization Theory and Applications* **55**, pp. 165-202.
- OBERLE H.J. (1976) Numerical Computation of Minimum-Fuel Space-Travel Problems by Multiple Shooting, Department of Mathematics, Munich University of Technology, Munich, Report M-7635.
- OBERLE H.J. (1977) On the Numerical Computation of Minimum-Fuel, Earth-Mars Transfer, *Journal of Optimization Theory and Applications* **22**, pp. 447-453.
- OBERLE H.J. (1982) Numerische Berechnung optimaler Steuerungen von Heizung und Kühlung für ein realistisches Sonnenhausmodell, Habilitationsschrift, Munich University of Technology, Munich.
- OBERLE H.J. AND GRIMM W. (1989) BNDSKO — A Program for the Numerical Solution of Optimal Control Problems, Internal Report No. 515-89/22, Institute for Flight Systems Dynamics, Oberpfaffenhofen: German Aerospace Research Establishment DLR.
- PESCH H.J. (1979) Numerical Computation of Neighboring Optimum Feedback Control Schemes in Real-Time, *Applied Mathematics and Optimization* **5**, pp. 231-252.
- PESCH H.J. (1980) Neighboring Optimum Guidance of a Space-Shuttle-Orbiter-Type Vehicle, *Journal of Guidance and Control* **3**, pp. 386-391.
- PESCH H.J. (1989A) Real-time Computation of Feedback Controls for Constrained Optimal Control Problems, Part 1: Neighbouring Extremals, *Optimal Control Applications and Methods* **10**, pp. 129-145.
- PESCH H.J. (1989B) Real-time Computation of Feedback Controls for Constrained Optimal Control Problems, Part 2: A Correction Method Based on Multiple Shooting, *Optimal Control Applications and Methods* **10**, pp. 147-171.
- PESCH H.J. (1990A) Optimal Re-Entry Guidance under Control and State Constraints, *Proceedings of the 8th IFAC Workshop on Control Applications of Nonlinear Programming and Optimization*, Paris, 1989, Edited by P. Bernhard and H. Bourdache-Siguerdidjane, IFAC Workshop Series, 1990, No. 2, Oxford: Pergamon Press, pp. 33-38.
- PESCH H.J. (1990B) Optimal and Nearly Optimal Guidance by Multiple Shooting, *Mécanique Spatiale — Space Dynamics*, Proceedings of the International Symposium, Toulouse, 1989, Edited by Centre National d'Etudes Spatiales, Toulouse: Cepadues Editions, pp. 761-771.
- PESCH H.J. Solving Optimal Control and Pursuit-Evasion Game Problems of High Complexity, *Proc. of the 9th IFAC Workshop on Control Applica-*

- tions of Optimization*, Munich, 1992, Edited by R. Bulirsch and D. Kraft, Basel: Birkhäuser (ISNM), to appear.
- PESCH H.J., SCHLEMMER M. AND VON STRYK O. Minimum-Energy and Minimum-Time Control of Three-Degrees-of-Freedom Robots, Part 1: Mathematical Model and Necessary Conditions, to appear.
- PESCH H.J., SCHLEMMER M. AND VON STRYK O. Minimum-Energy and Minimum-Time Control of Three-Degrees-of-Freedom Robots, Part 2: Numerical Methods and Results for the Manutec r3 Robot, to appear.
- SÄNGER E. (1962) Raumfahrt — gestern, heute und morgen, *Astronautica Acta* **VIII** 6, pp. 323-343.
- SCHARMACK D.K. (1967) An Initial Value Method for Trajectory Optimization Problems, *Advances in Control Systems* 5, Edited by C. T. Leondes, New York: Academic Press, pp. 1-65.
- SHAU G.-C. (1973) Der Einfluß flugmechanischer Parameter auf die Aufstiegsbahn von horizontal startenden Raumtransportern bei gleichzeitiger Bahn- und Stufungsoptimierung, Dissertation, Department of Mechanical and Electrical Engineering, University of Technology, Braunschweig.
- STOER J. AND BULIRSCH R. (1980) Introduction to Numerical Analysis, Springer: New York (2nd Edition, 1993).
- VON STRYK O. AND SCHLEMMER M. Optimal Control of the Industrial Robot Manutec r3, *Proceedings of the 9th IFAC Workshop of Control Applications of Optimization*, Edited by R. Bulirsch and D. Kraft, International Series of Numerical Mathematics, Basel: Birkhäuser.
- VON STRYK O. AND BULIRSCH R. (1992) Direct and Indirect Methods for Trajectory Optimization, *Annals of Operations Research* 37, pp. 357-373.